Electronic Supplementary Material (ESI) for RSC Advances.

Supporting Information

Dinuclear salen Cobalt complex incooperated $Y(OTf)_3$: Enhanced enantioselectivity in hydrolytic kinetic resolution of epoxides

Deepak Patel,[a] Ganesh RamKurrey,[a] Sandip S. Shinde,[b] Pradeep Kumar,[b] Geon-Joong Kim[c] and Santosh Singh Thakur[a]*

[a]*Department of Chemistry. Guru Ghasidas Vishwavidyalaya , Koni, Bilaspur, Chhattisgarh, India Fax: +917752 260435; Tel: +919981209738; E-mail: santosh.chirality@gmail.com*

[b] *Organic Chemistry Division; National Chemical Laboratory, Dr. Homi Bhabha Road, Pune 411008, India*

[c] *Department of Chemical Engineering, Inha University, Incheon, Republic of Korea*

Table of contents

I. General: Instruments, chemicals

II. Catalyst preparation

III. Reaction method and kinetic measurements

IV. UV-vis and calculation of ε and concentration of [Co^{II}] and [Co^{III}]

V. Characterization data of catalyst: ^{1}H, ^{13}C and ^{19}F NMR, IR, XRD elemental analysis

VI. Table for optically active diol.

VII. Characterization recovered epoxides and diols

VIII. Gas chromatogram of recovered epoxides and diols

IX. Recycling method

X. References

I.

General

Instruments

^{19}F NMR were recorded using 376.3 MHz at 9.3 T and ^{1}H and ^{13}C by 400 MHz, NMR spectrometer (Bruker, UltraShield). Gas Chromatography analyses were performed on 7890 B Agilent instruments equipped with FID detector and LabChem software for data analysis. UV spectra were recorded on UV-VIS double beam spectrophotometer (SHIMADZU 1800) interfaced with PC using UV probe 2.34 software for data analysis. The FT IR (Bruker Alpha Model), XRD ('X' pert Pro), Mass by Q-Exactive HRMS (Themoscientific), Optical rotation by digital polarimeter (JASCO P-2000). Chiral GC (Agilent 7890B) or chiral HPLC were used for the analysis of reaction mixture. G-TA chiral column (Astec® Chiraldex® 30 m × 0.25 mm x 0.12 μm), α-TA and Chiralcel OD-H were used for separation. The recovered epoxide was confirmed by ^{1}H, ^{3}C NMR, elemental analysis and GC-MS. The product and epoxides were separated using Kugelrohr distillation (Buchi, Glass Oven B-585 Kugelrohr).

Chemicals

(*R, R*)- (-)-N, N′-bis (3,5-di-tert-butylsalicylidene)-1,2-cyclohexane diamino cobalt (II), Y(OTf)$_3$ procured from Aldrich and racemic epoxides were either purchased from Aldrich or TCI and used as such. Solvents were used after distillation

II

Catalyst preparation

Monomer

An oven dried 50 mL flask equipped with a stir bar was charged with (*R,R*)- salen Co (4.0 g, 6.63 mmol,1.0 equiv.) was stirred in THF (20 mL) at open atmosphere at room temperature. Yttrium triflate (4.73 g, 8.82 mmol, 1.33 equiv.) was added to a stirred solution of chiral salen Co (II) **1**. As the reaction proceeds the colour of the solution changes from brick red to dark green. The solution was stirred at room temperature for 40 minutes. After completion of reaction the solvent was removed by rotary evaporation and crude green solid residue was dried. The crude green solid was worked up with H_2O and CH_2Cl_2. Yield = > 98 %; dark green solid powder (m. p. > 380^{o}C). The reaction progress was continuously monitored UV-vis spectrophotometer. The catalyst is characterized by XRD, XPS, FTIT, ^{1}H, ^{13}C ^{19} F NMR (solvent $CDCl_3$).

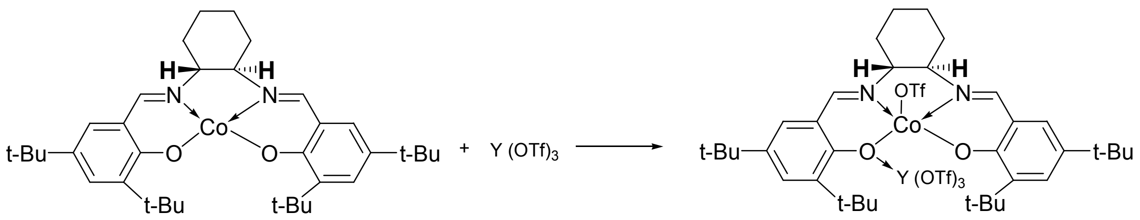

1.00 1.33 equiv.

1 Salen Co-^{III}Y(OTf)$_3$-**Monomer catalyst A**

Dimer

An oven dried 50 mL flask equipped with a stir bar was charged with (*R,R*)- salen Co (4.0 g, 6.63 mmol, 2.0 equiv.) was stirred in THF (20 mL) at open atmosphere at room temperature. Yttrium triflate (2.95 g, 5.503 mmol, 1.66 equiv.) was added to a stirred solution of chiral salen Co (II) **1**. As the reaction proceeds the colour of the solution changes from brick red to dark green. The solution was stirred at room temperature for 40 minutes. After completion of reaction the solvent was removed by rotary evaporation and crude green solid residue was dried. The crude green solid was worked up with H_2O and CH_2Cl_2. Yield = > 98 %; dark green solid powder (m. p. > 380°C). The reaction progress was continuously monitored UV-vis spectrophotometer. The catalyst is characterized by XRD, XPS, FTIR, ^{1}H, ^{13}C,^{19} F NMR (solvent $CDCl_3$) and elemental analysis.

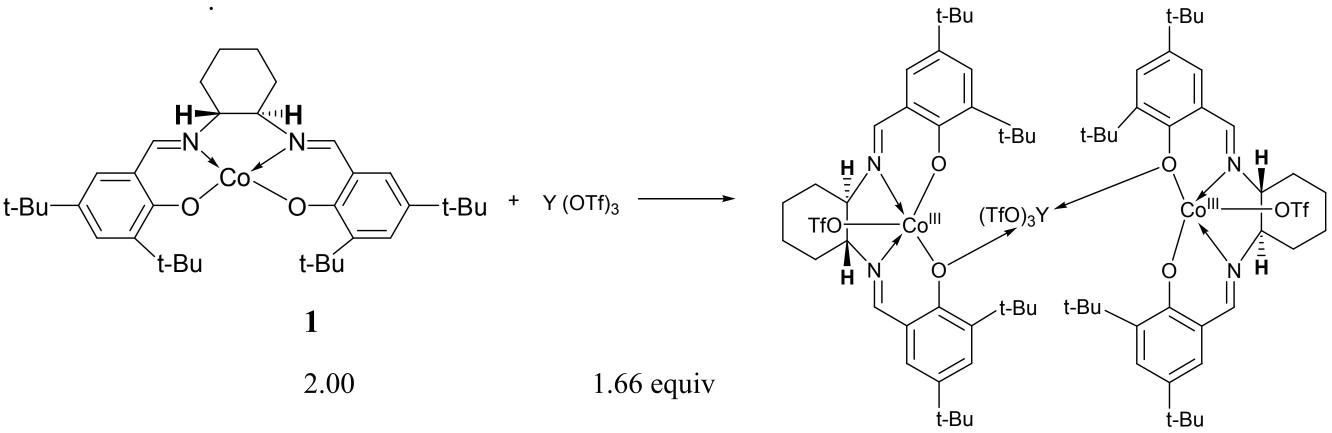

1

Salen Co-^{III}(YOTf)$_3$-**Dinuclear catalyst B**

III

Reaction Method

An oven dried 5 mL flask equipped with a stir bar was charged with (*R,R*)-dinuclear catalyst B (0.2 mol %,) and (±)-epichlorohydrine (1.002 g, 10.84 mmol) was stirred at open atmosphere at room temperature. H_2O (0.1073 g, 5.96 mmol. 0.55 equiv.) was added. The reaction was mildly exothermic. The reaction mixture was stirred for 4 hours. The reaction mixture was checked periodically by using Chiral GC or chiral HPLC. Similarly same molar ratio was taken for entry all the entries.

Kinetic experiment[1-4]

20 mL vials were charged with a stir bar and 0.08 mmol dimer catalyst B and 0.16 m mol for monomer catalyst A. The catalyst were dissolved in THF (5.00 mL), then (*rac*)-ECH (3.70 mL, 40 mmol) and bromobenzene (250 µL; as an internal standard) were added to solution. After the mixture had been stirred for 1 h at 25 °C, water (0.39 mL, 22 mmol) was added. Initial rate of the reaction conversion was monitored by GC analysis of 20 µL aliquots withdrawn periodically from the reaction mixture. Even though the reactions were kinetically well-behaved over several half-lives, initial rates were used to avoid complications.

IV. UV-vis and calculation of ε and concentration of [Co^{II}] and [Co^{III}]

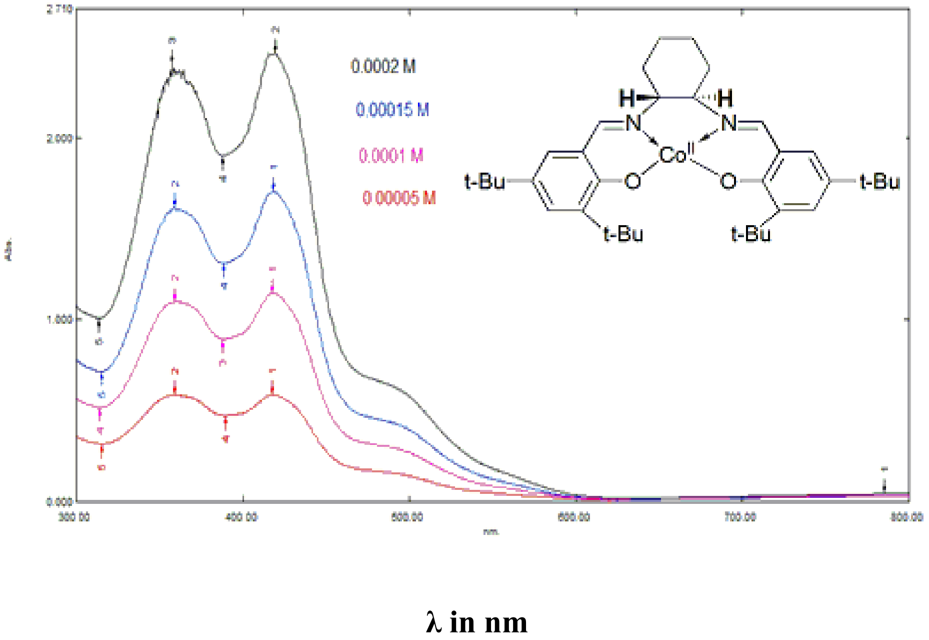

Figure S1: UV-vis spectra of Chiral Salen Co^{II} (Salen= *N,N′*-bis(3,5-di-tert-butylsalicylidene)-1,2-cyclohexane-diamine)at different concentration for the calculation of ε.

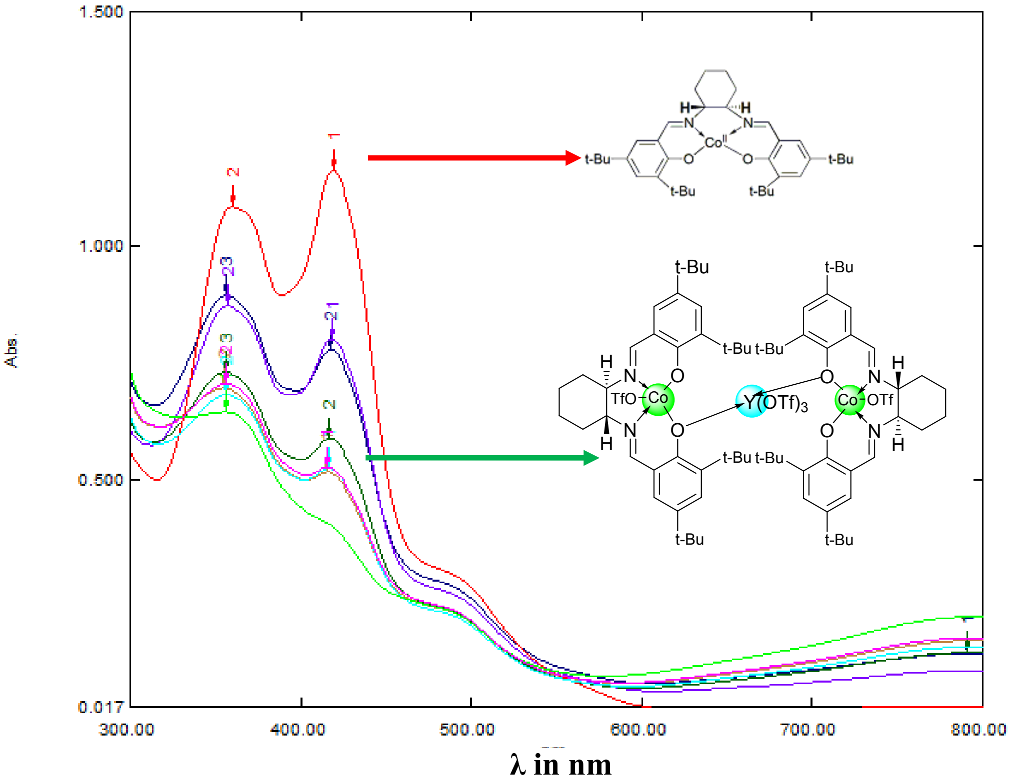

Figure S2: Continuous monitoring of UV-vis spectra for the formation of dimer chiral salen Co^{II} (Salen= *N,N′*-bis (3,5-di-tert-butylsalicylidene)-1,2-cyclohexane-diamine) at different time interval

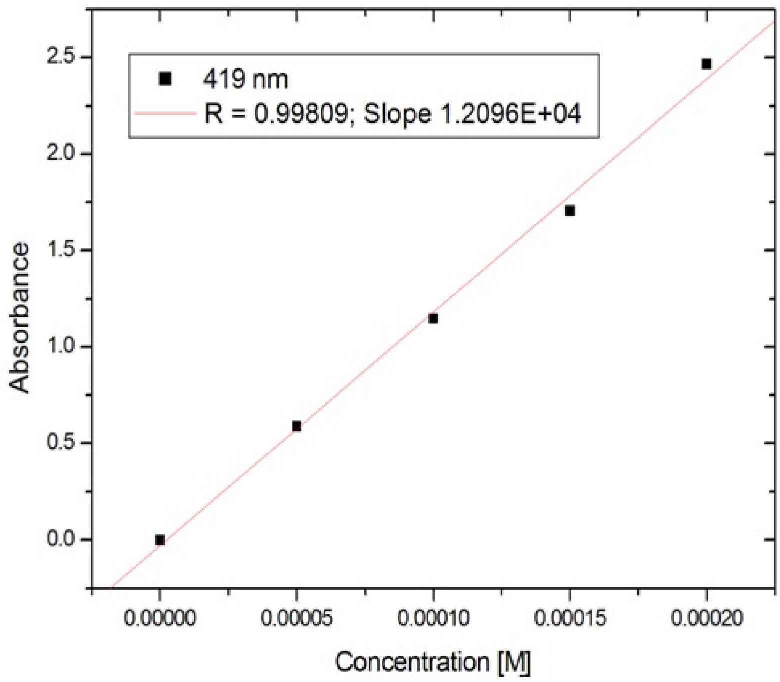

Figure S3: Linear regression analysis of chiral salen Co ^{II} at 419 nm for the calculation of ε.

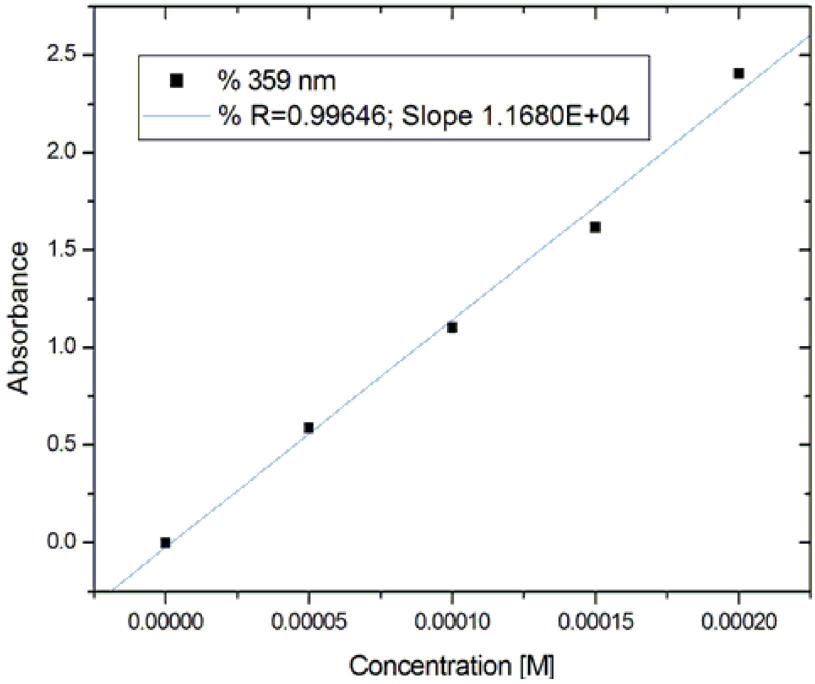

Figure S4: Linear regression analysis of chiral salen Co ^{II} at 419 nm for the calculation of ε.

The numerical calculation was done by using the Peng et al method.[5]

Through linear regression method, the values of molar extinction coefficient (ε) for Co^{II}–salen is caluculated at 419 nm and 359 nm are as:

ε at 359 = 1.168 E +04
ε at 419 = 1.209 E +04

The concentration of cabalt(II) salen $[Co^{II}]_0$ can be calculated by the measured molar extinction coefficient and applying Lambert Beer's law:
A = ε c l
For different times (0, 2, 6, 10, 20, 30, 40 mins.), the value of $[Co^{II}]$ at 419 can be given as:

$\varepsilon_{Co}II,_{419nm} \times [Co^{II}]_0 = Abs_{0,419nm}$
$[Co^{II}]_0 = 9.606$ E -5
$[Co^{II}]_2 = 6.448$ E -5 moles

$[Co^{II}]_6 = 4.877$ E -5 moles

$[Co^{II}]_{10} = 4.282$ E -5 moles

$[Co^{II}]_{20} = 3.480$ E -5 moles

$[Co^{II}]_{30} = 2.86$ E -5 moles

$[Co^{II}]_{40} = 0$

Because the absorbance of Co^{III}-R at 419 nm is much smaller and ultimately disappears at λ = 419 nm than that of 359 nm, we assume that absorbance of Co^{III}-R at 419nm is 0, to obtain $[Co^{III}]_2$ as:

$[Co^{III}]_2 = [Co^{II}]_0 - [Co^{II}]_2$

$[Co^{III}]_2$ = (9.606 E -5) – (6.448 E -5) = 3.158 E -5 moles

$[Co^{III}]_6$ = (9.606 E -5) – (4.877 E -5) = 4.729 E -5 moles

$[Co^{III}]_{10}$ = (9.606 E -5) – (4.282 E -5) = 5.324 E -5 moles

$[Co^{III}]_{20}$ = (9.606 E -5) – (3.480 E -5) = 6.126 E -5 moles

$[Co^{III}]_{30}$ = (9.606 E -5) – (2.860 E -5) = 6.746 E -5 moles

$[Co^{III}]_{40}$ = (9.606 E -5) – 0 = 9.606 E -5 moles

The summary is as follows,

Table S1- The conversion of salen-Co^{II} to salen Co^{III} by Y(OTf)$_3$ (Dimer)

Entry	Time (In Mints) .)	[Co^{II}]$_t$	[Co^{III}]$_t$
1	0	0.00009606	0
2	2	0.00006448	0.00003158
3	6	0.00004877	0.00004729
4	10	0.00004282	0.00005324
5	20	0.00003480	0.00006126
6	30	0.00002860	0.00006746
7	40	0	0.00009606

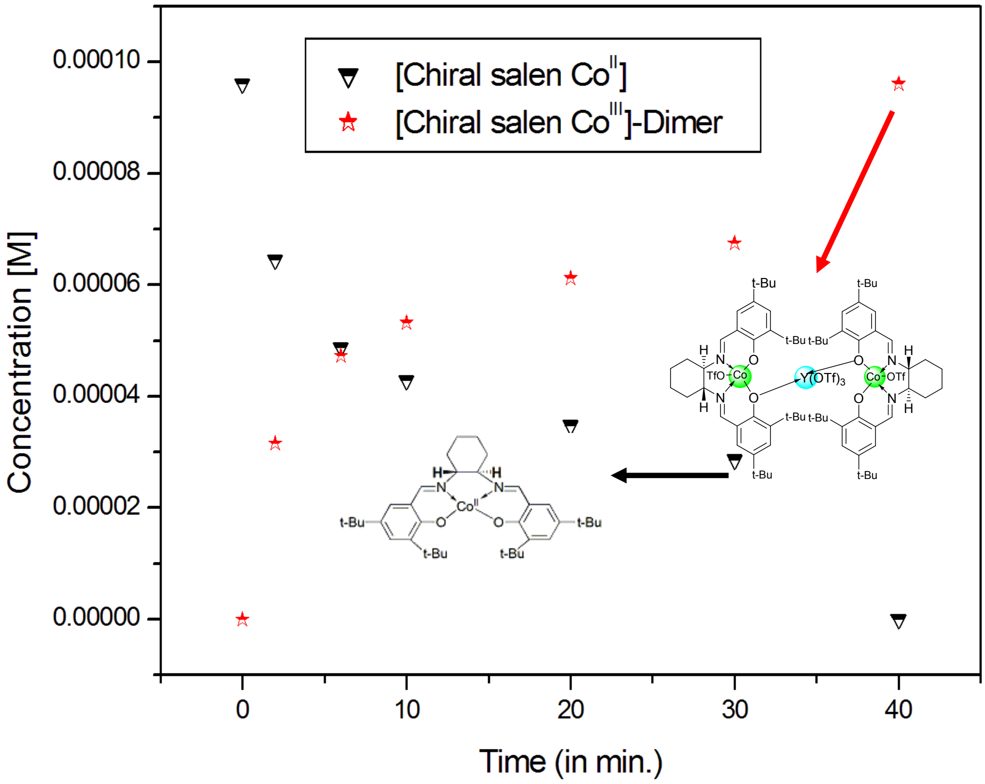

Figure S5: The change of concentration of salen Co^{II} to salen Co^{III}-dimer B as a function of time.

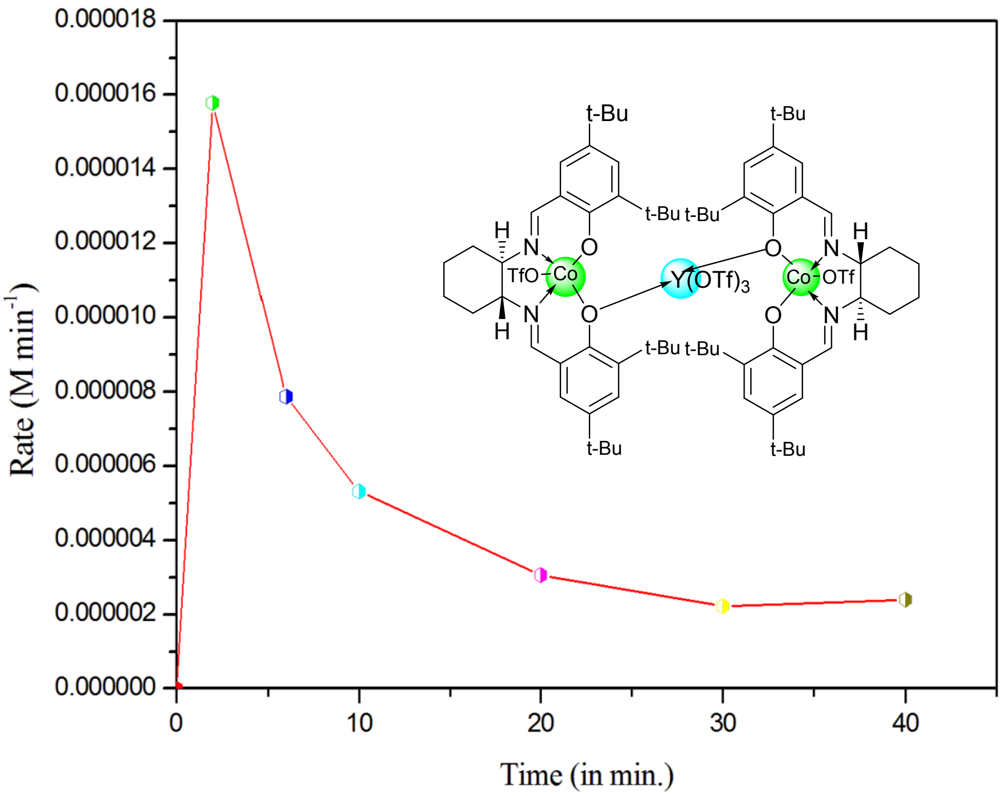

Figure S6-: Kinetic profile for the formation of chiral salen Co^{III}- $Y(OTf)_3$.

V. Characterization data of catalyst: ^1H, ^{13}C, ^{19}F NMR, IR, XRD and elemental anaysis

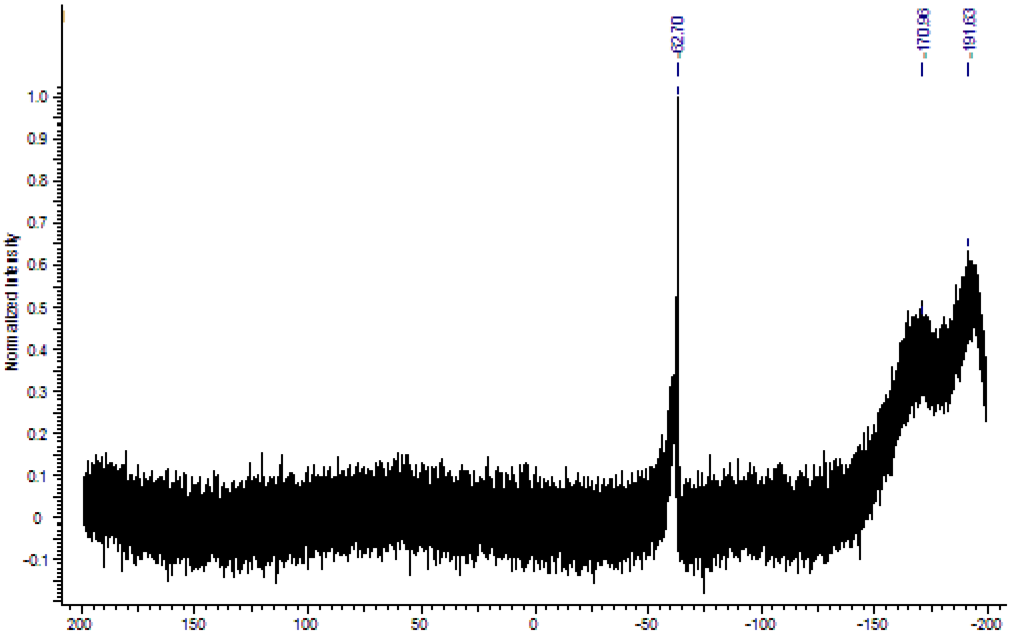

Figure S7: ^{19}F NMR of chiral salen Co- $Y(OTf)_3$ dimer catalyst B.

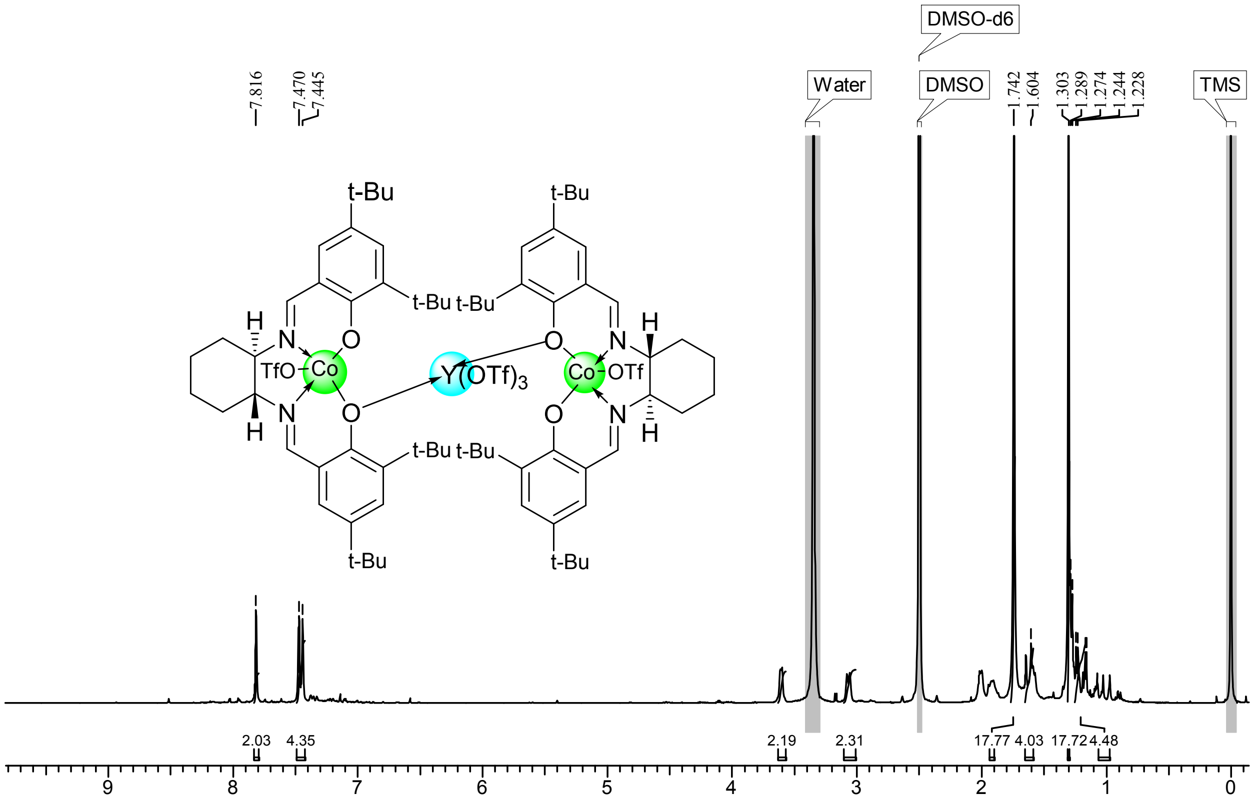

Figure S8: ^{1}H NMR of chiral salen Co- Y(OTf)$_3$ dimer catalyst B.

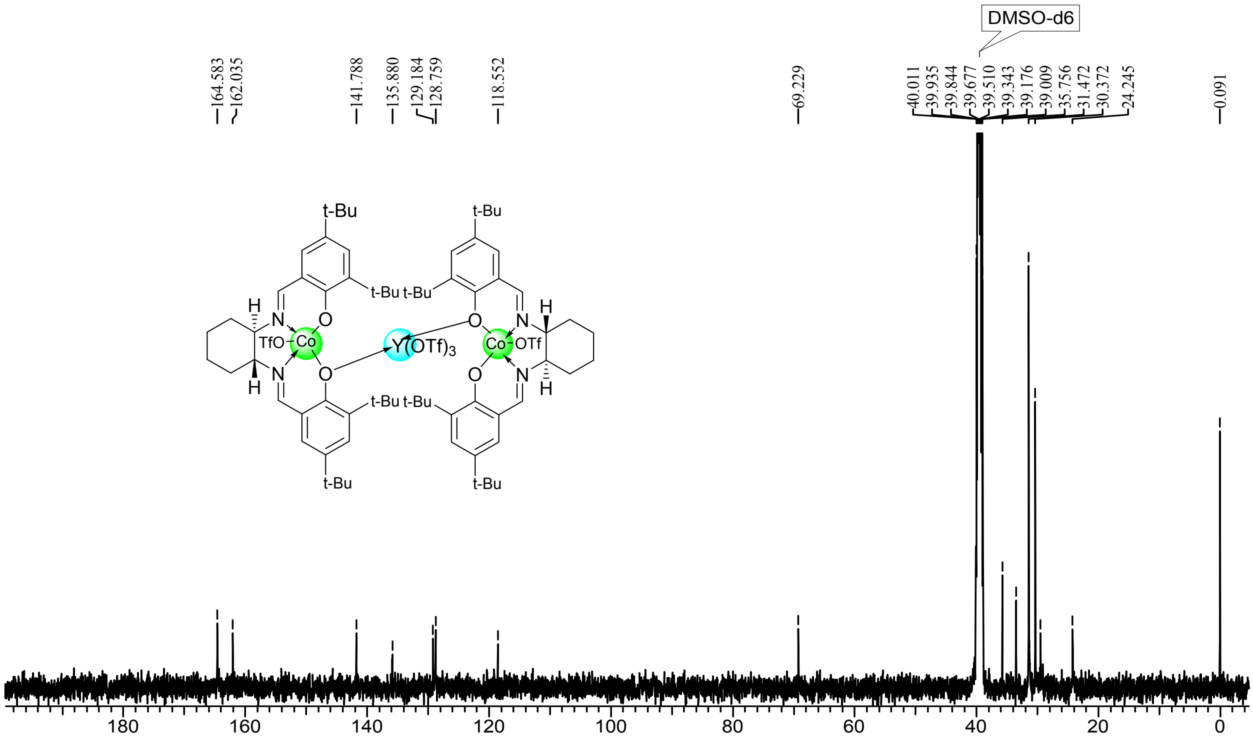

Figure S9: ^{13}C NMR of chiral salen Co- Y(OTf)$_3$ dimer catalyst B.

Cobalt-Dimer-Y(OTf)$_3$Complex; solid, ^{1}H NMR (400 MHz, $CDCl_3$) δ 1.22-1.28(m, 8H), 1.30(s, 36H), 1.74(s, 36H), 1.60(m, 8H), 3.1(s, 4H), 3.7(s, 4H), 7.45(d, J = 10Hz, 8H), 7.8 (s, 4H); ^{13}C NMR (100 MHz, $CDCl_3$) δ 24.2, 30.3, 31.4, 35.7, 39.0, 69.2, 118.5, 128.7, 129.1, 135.8, 141.7, 162.0, 164.5. Anal (%). Calcd for $C_{78}H_{106}F_{15}N_4S_5Co_2YO_{19}$: C,45.57; H,5.20; F,13.86; N, 2.73; S, 7.80; Co,5.73; Y, 4.32. Found: C,46.45; H,4.88; F,14.22; N, 3.03; S, 8.12; Co,6.80; Y, 5.20; HRMS (EI) calcd for $C_{77}H_{104}Co_2F_{15}N_4O_{19}S_5Y$ (M^+) 2040.3381, found 2041.3415.

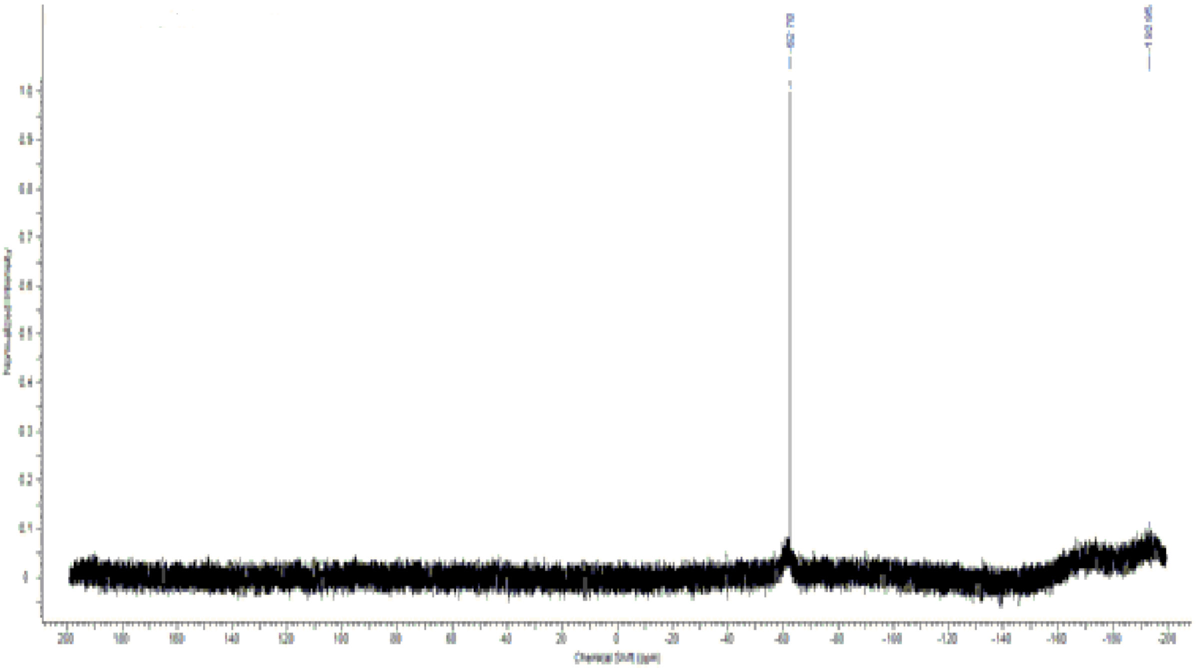

Figure S10 : ^{19}F NMR of chiral salen Co-Y(OTf)$_3$ monomer catalyst A.

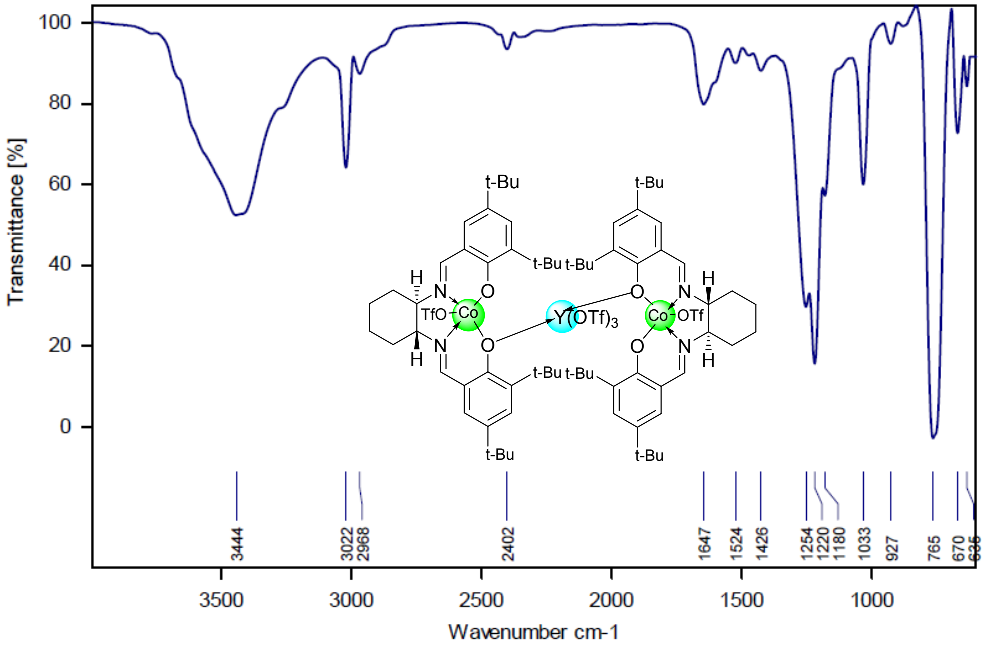

Figure S11: FT-IR of chiral salen Co- Y(OTf)$_3$ dimer catalyst B

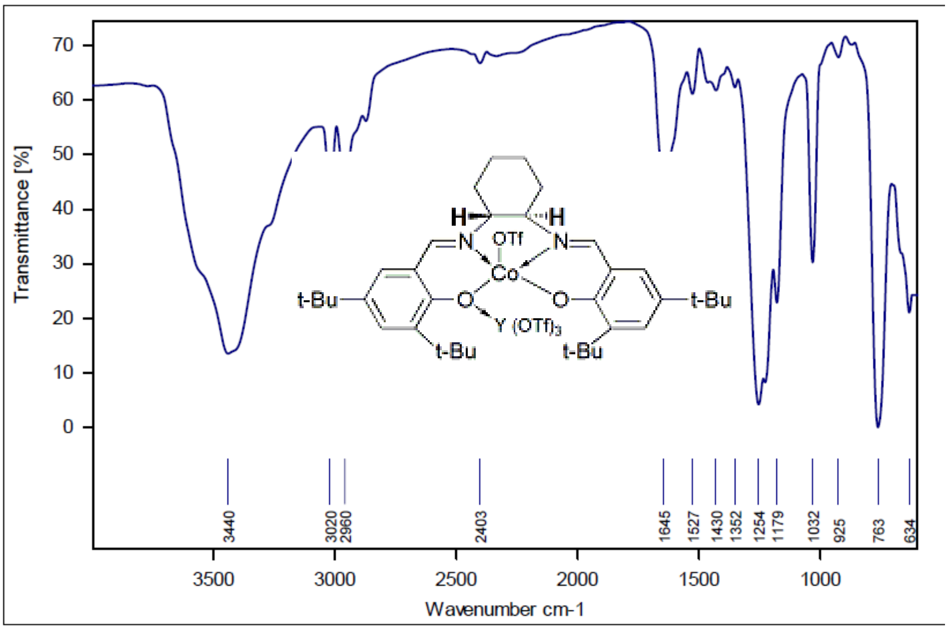

Figure S12: FTIR of chiral salenCo- Y(OTf)$_3$ monomer catalyst A

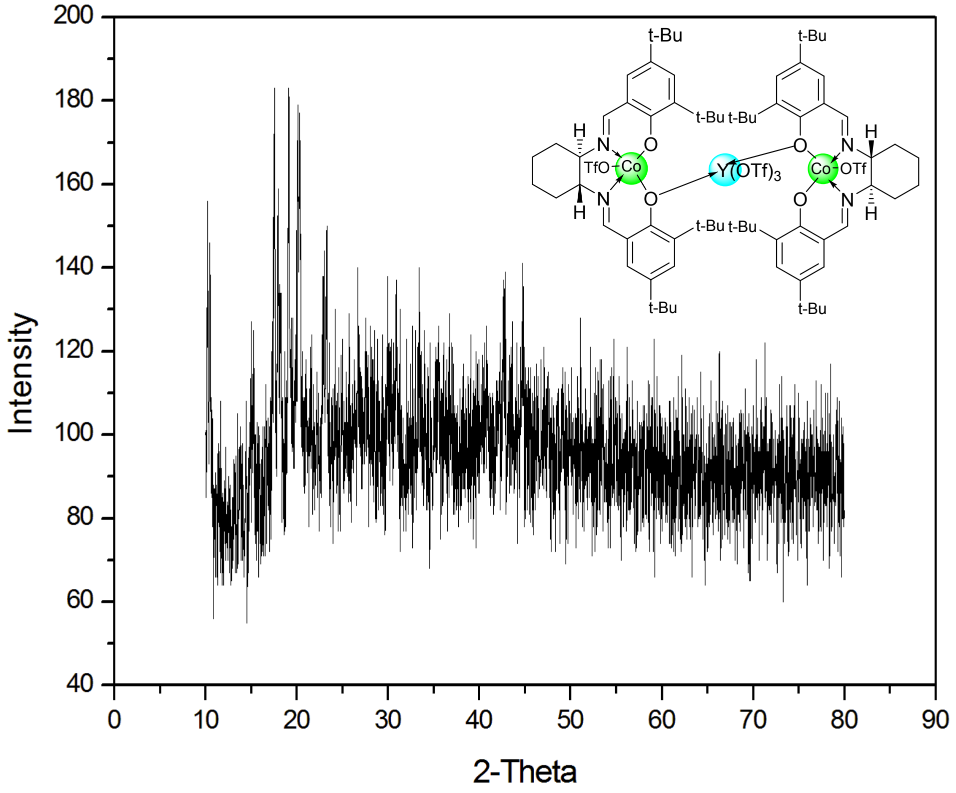

Figure S13: Powder XRD of chiral salen Co- Y(OTf)$_3$ dimer catalyst B

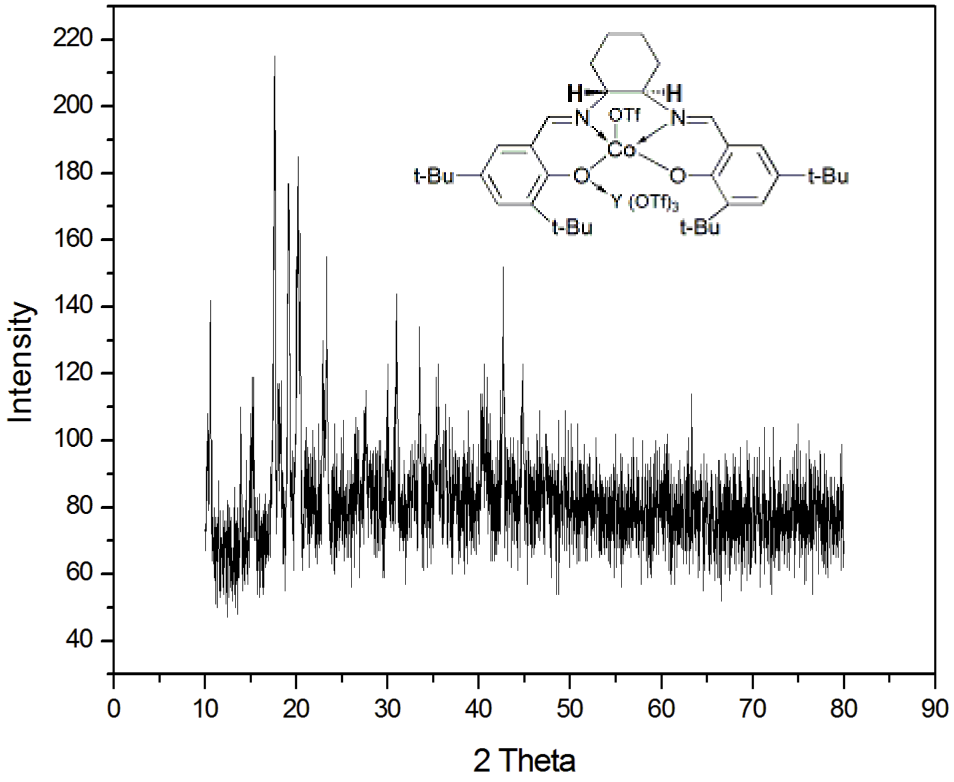

Figure S14: Powder XRD of chiral salen Co- Y(OTf)$_3$ monomer catalyst B

VI-Table S-2. HKR of terminal epoxides catalyzed by the mono and bi-metallic catalyst A and B.

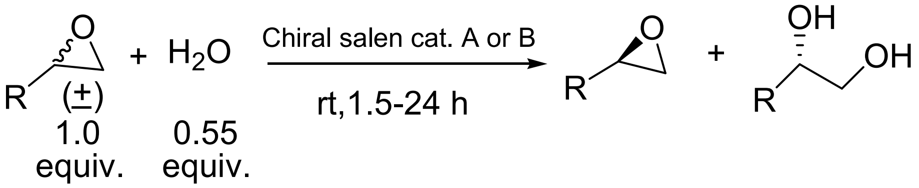

Entry	Isolated Product	Catalyst type[a]	Time (h)	% Yield (ee) [b]
1	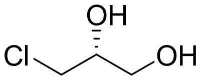	A	12	21 (46.2)
		B	4	45 (88.1)
2	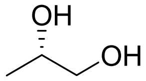	A	6	21 (51.3)
		B	2	41 (89.4)
3	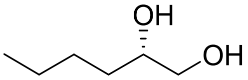	A	16	23 (69.7)
		B	10	42 (91.8)
4	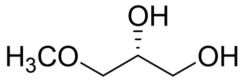	A	12	19 (48.2)
		B	1.5	42 (88.5)
5	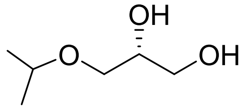	A	12	21(21.3)
		B	1.5	41 (90.9)
6	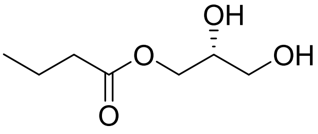	A	12	
		B	2	41 (88.3)
7[c]	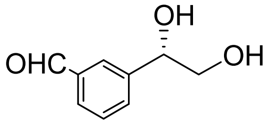	A	12	11 (29)
		B	6	38 (86.1)
8[d]	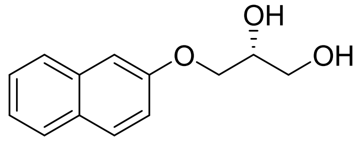	A	12	11 (29)
		B	6	38 (86.1)

---

[a] Catalyst loading based on racemic epoxides and for A =0.4 mol%; B=0.2 mol%. [b] ee % was determined by chiral GC or chiral HPLC. And isolated yield is based on racemic epoxides (theoretical maximum=50%). [d] Solvent THF: CH_2Cl_2 2:1 (v/v) with respect to epoxides. [e] THF is used as solvent.

VII Characterization of recovered epoxides and diols

^{1}H and ^{13}C NMR of epoxides (Table 1 MS)

Entry 1. Epichlorohydrin, The *ee* of the epichlorohydrine was determined by chiral GC >99%; ^{1}H NMR (400 MHz, CDCl$_3$) δ 3.58-3.35 (m, 2H), 3.26-3.22(m, 1H), 2.88(dd, *J* = 9.2 Hz, 1H), 2.67(dd, *J* = 4.1Hz, 1H), ^{13}C NMR (100 MHz, CDCl$_3$) δ 51.1, 46.8, 45.0; HRMS (EI) calcd for C_3H_5ClO (M$^+$) 92.0029, found 92.0027 [α]^{20}D + 33.5 (c=1,CH_3OH) compared with standard product.

Entry 2. 2-methyloxirane; ^{1}H NMR (400 MHz, CDCl$_3$) δ 2.96 (m, 1H), 2.73 (dd, *J* = 1.8, 17.1Hz, 1H), 2.41(dd, *J* =1.8, 9.3Hz, 1H), 1.30 (d, *J* = 6.2Hz, 1H) ^{13}C NMR (100 MHz, CDCl$_3$) δ 48.9, 47.95, 17.91. HRMS (EI) calcd for C_3H_6O (M$^+$) 58.0419, found 58.0419 [α]^{20}D – 14.3 ; compared with standard product.

Entry 3. 2-butyloxirane: ^{1}H NMR (400 MHz, CDCl$_3$) δ 2.88-2.74 (m, 1H), 2.71(dd, *J* =1.4Hz, 1H), 2.44(dd, *J* = 1.4Hz, 1H), 1.50-1.34 (m, 8H), 0.90 (t, *J* =6.7 Hz, 1H); ^{13}C NMR (100 MHz, CDCl$_3$) δ 52.3, 46.9, 32.2, 28.3, 27.94, 22.35, 13.80. HRMS (EI) calcd for $C_6H_{12}O$ (M$^+$) 100.09, found 100.07. [α]^{20}D – 10.1; compared with standard product.

Entry 7. 4-(oxiran-2-ylmethoxy)benzaldehyde: ^{1}H NMR (400 MHz, CDCl$_3$) δ 9.9 (s, 1H) 7.87 (d, *J* = 8.1Hz, 1H), 7. 0 (d, *J* =8.1Hz 1H), 4.34-4.36 (m, 1H), 4.00-4.04 (m, 2H), 3.38 (dd, J = 2.4, 5.6Hz, 1H) 2.95-2.93 (dd, J = 1.4, 4.8Hz, 1H); ^{13}C NMR (100 MHz, CDCl$_3$) δ 190.7, 163.1, 132.0, 130.5, 114.8, 69.6, 68.7, 45.8; HRMS (EI) calcd for $C_{10}H_{10}O_3$ (M$^+$) 178.0630, found 178.0626.

Entry 8. 2-[naphthalene-2-yloxy)methyl]oxirane; ^{1}H NMR (400 MHz, CDCl$_3$) δ 7.86-7.71 (m, 3H), 7.45-7.35 (m, 2H), 7.21-7.14 (m, 2H), 4.37 (dd, *J* = 4.2, 7.3 Hz, 1H), 4.09 (dd, *J* = 4.3, 7.3 Hz, 1H), 3.45-3.43 (m, 1H), 2.95 (t, *J* = 4.1 Hz, 1H), 2.83 (dd, *J* = 2.6, 3.0 Hz, 1H); ^{13}C NMR (400 MHz, CDCl$_3$) δ 154.4, 134.6, 129.5, 129.1, 127.3, 126.7, 126.4, 123.8, 118.7, 106.8, 68.72, 50.11, 44.78. HRMS (EI) calcd for $C_{13}H_{12}O_2$ (M$^+$) 200.0837, found 200.0840.

^{1}H and ^{13}C NMR of diols (Table S2)

Entry 1. Epichlorohydrin diol; ^{1}H NMR (400 MHz, CDCl$_3$) δ 4.61-4.53(m, 2H), 4.18 (m, 1H), 3.70-3.62 (m, 1H), ^{13}C NMR (400 MHz, CDCl$_3$) δ 72.8, 67.8, 45.3.

Entry 3. hexane-1,2-diol; ^{1}H NMR (400 MHz, CDCl$_3$) δ 4.05 (bs, 2 H), 3.64 (m, 1H), 3.56 (dd, *J* = 1.6Hz, 1H), 3.37 (dd, *J* = 1.6, 10.1Hz, 1H), 1.39-1.28 (m, 8H), 0.90 (t, *J* = 6.7Hz, 3H); ^{13}C NMR (100 MHz, CDCl$_3$) δ 72.1, 66.4, 32.7, 27.8, 27.7, 22.6, 13.8. HRMS (EI) calcd for $C_7H_{16}O_2$ (M$^+$) 118.0994, found 118.0920.

Entry 8. 3-(naphthalene-2-yloxy)propane-1,2-diol; ^{1}H NMR (400 MHz, CDCl$_3$) δ 7.801 7.74 (m, 3H,), 1.79 (br, 2H, OH), 7.48-7.40 (m, 2H,), 7.38-7.15 (m, 2H,), 4.72- 4.70 (m, 2H,) 4.40 (m, 1H), 4.20- 4.17 (m, 2H); ^{13}C NMR (400MHz, CDCl$_3$) δ 155.8, 134.7, 129.7, 129.2, 127.6, 126.8, 126.6, 123.1, 118.3, 106.9, 73.1, 68.2, 67.1. HRMS (EI) calcd for $C_{13}H_{14}O_3$ (M$^+$) 218.0943, found 218.0939.

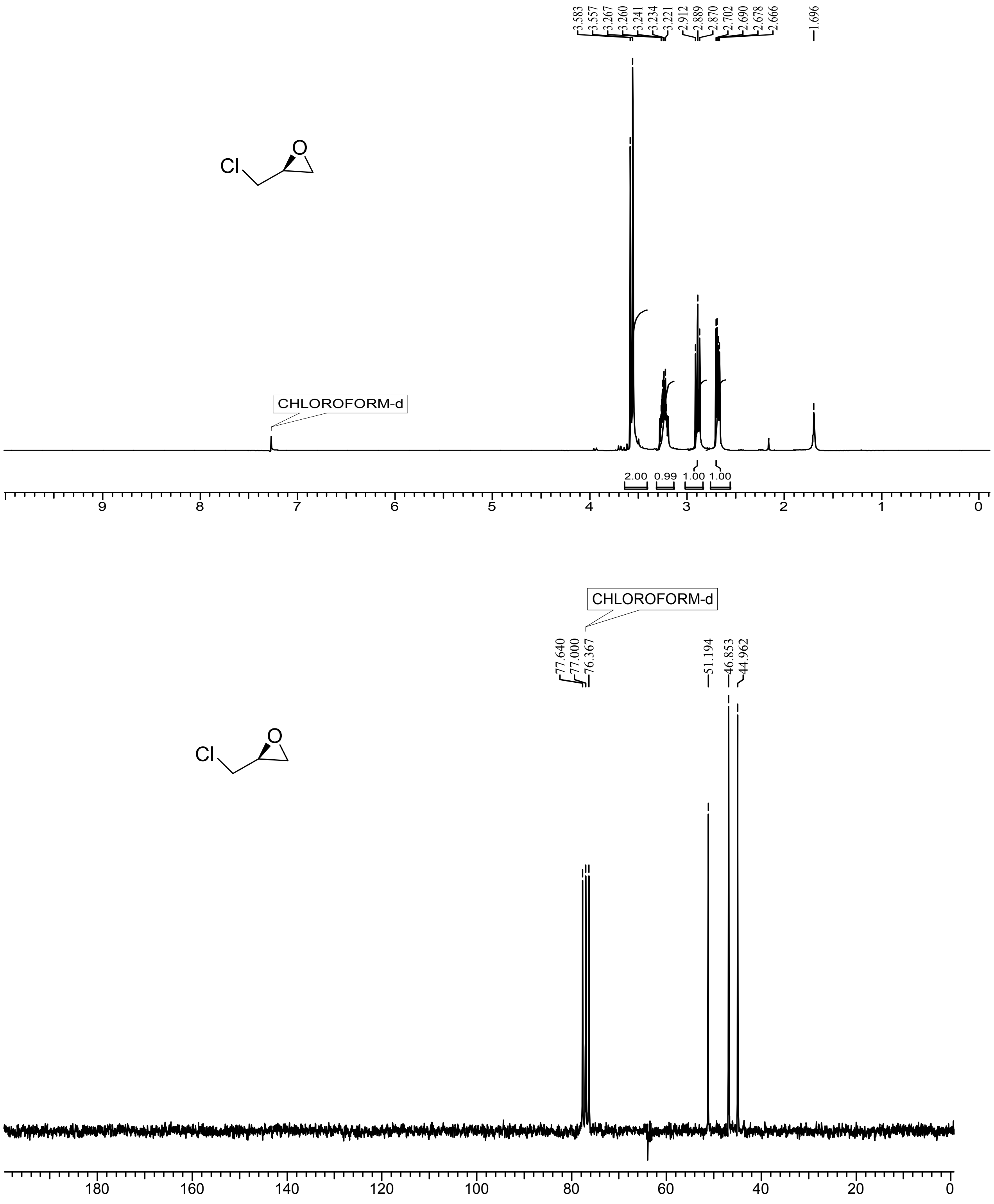

Figure S15: ^{1}H & ^{13}C NMR (*S*)-epichlorohydrine

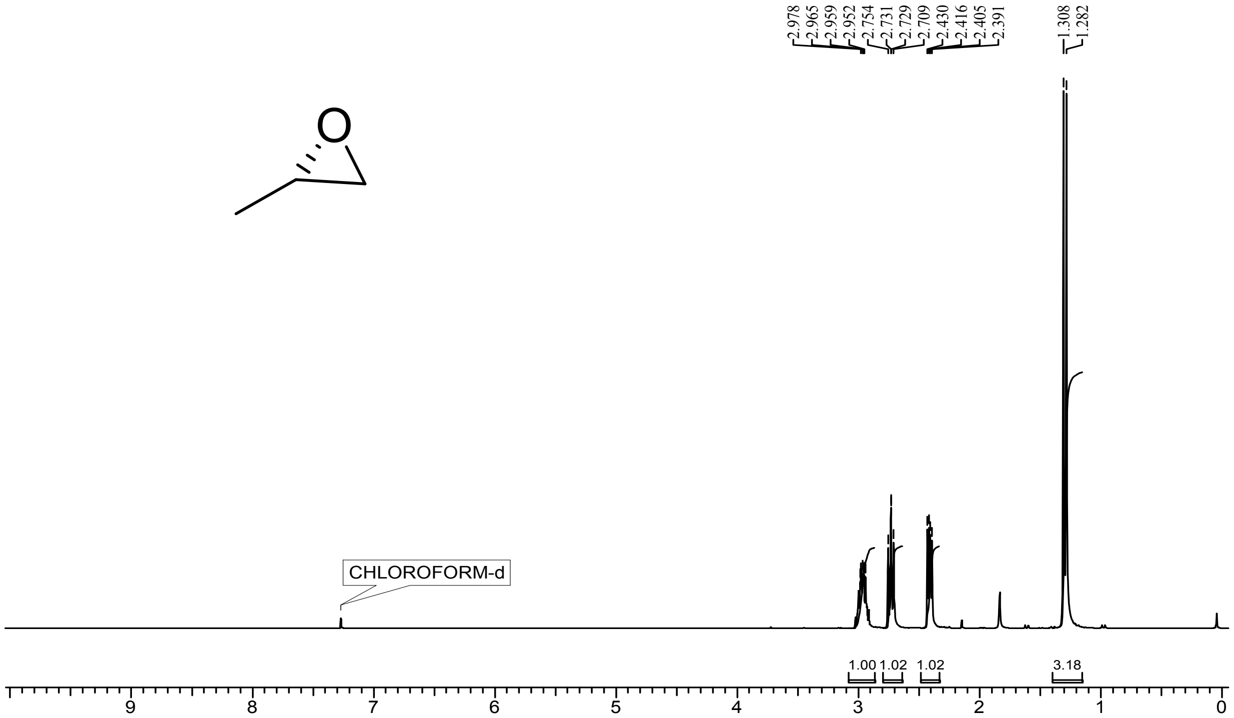

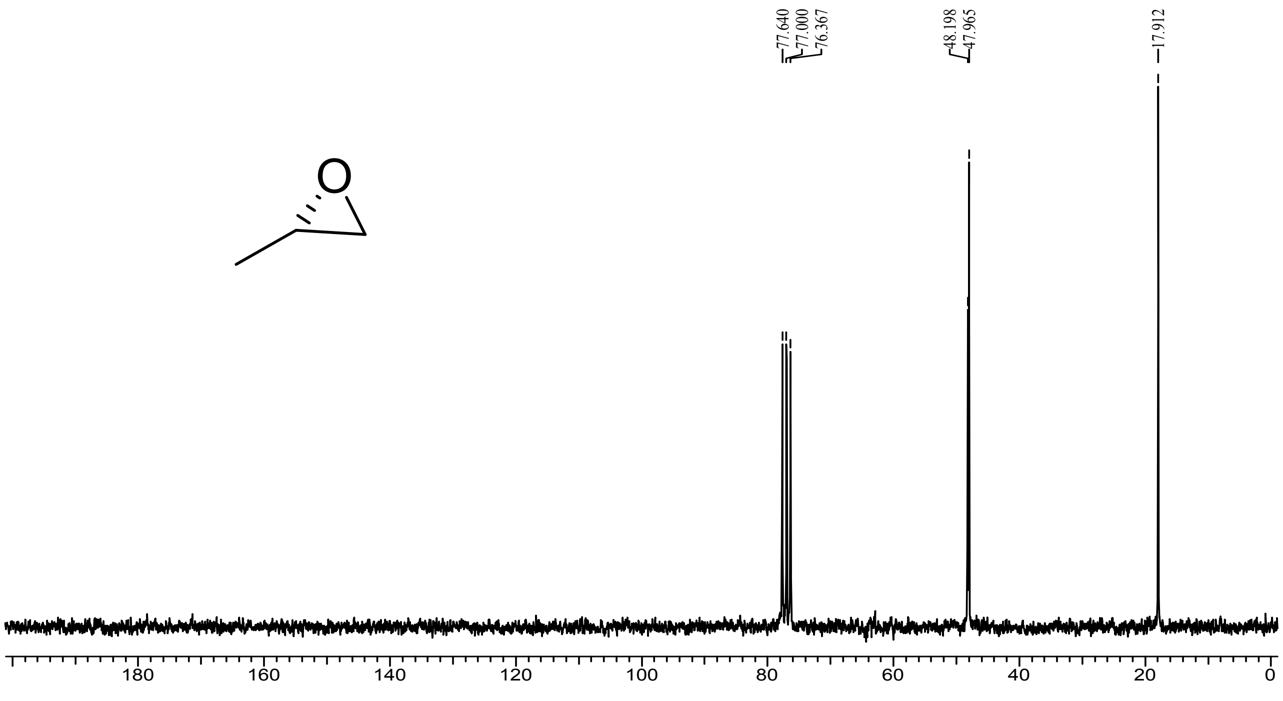

Figure S16: ^{1}H and ^{13}C NMR (*S*)-2-methyloxirane

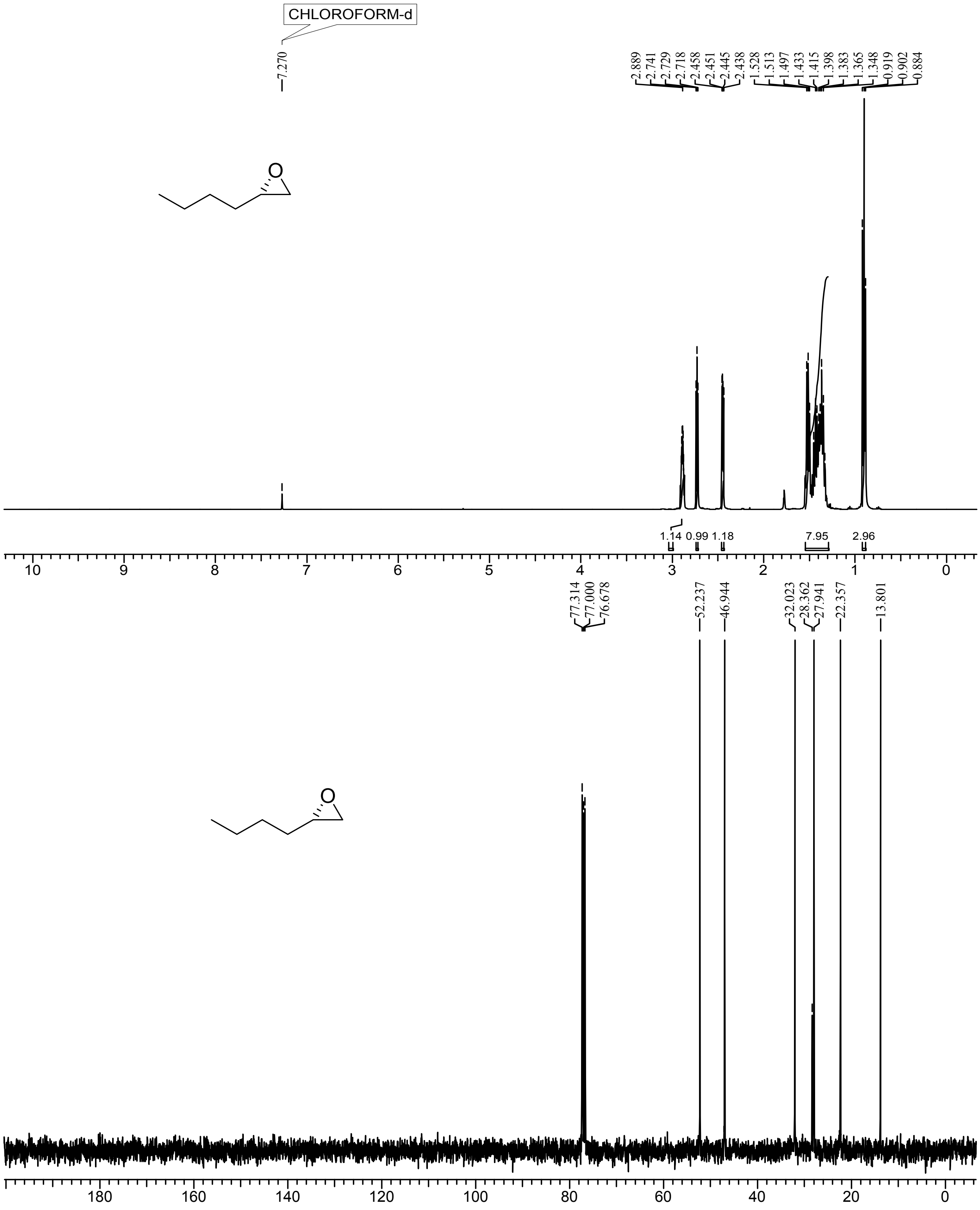

Figure S17: ^{1}H and ^{13}C NMR (*S*) 2-butylloxirane

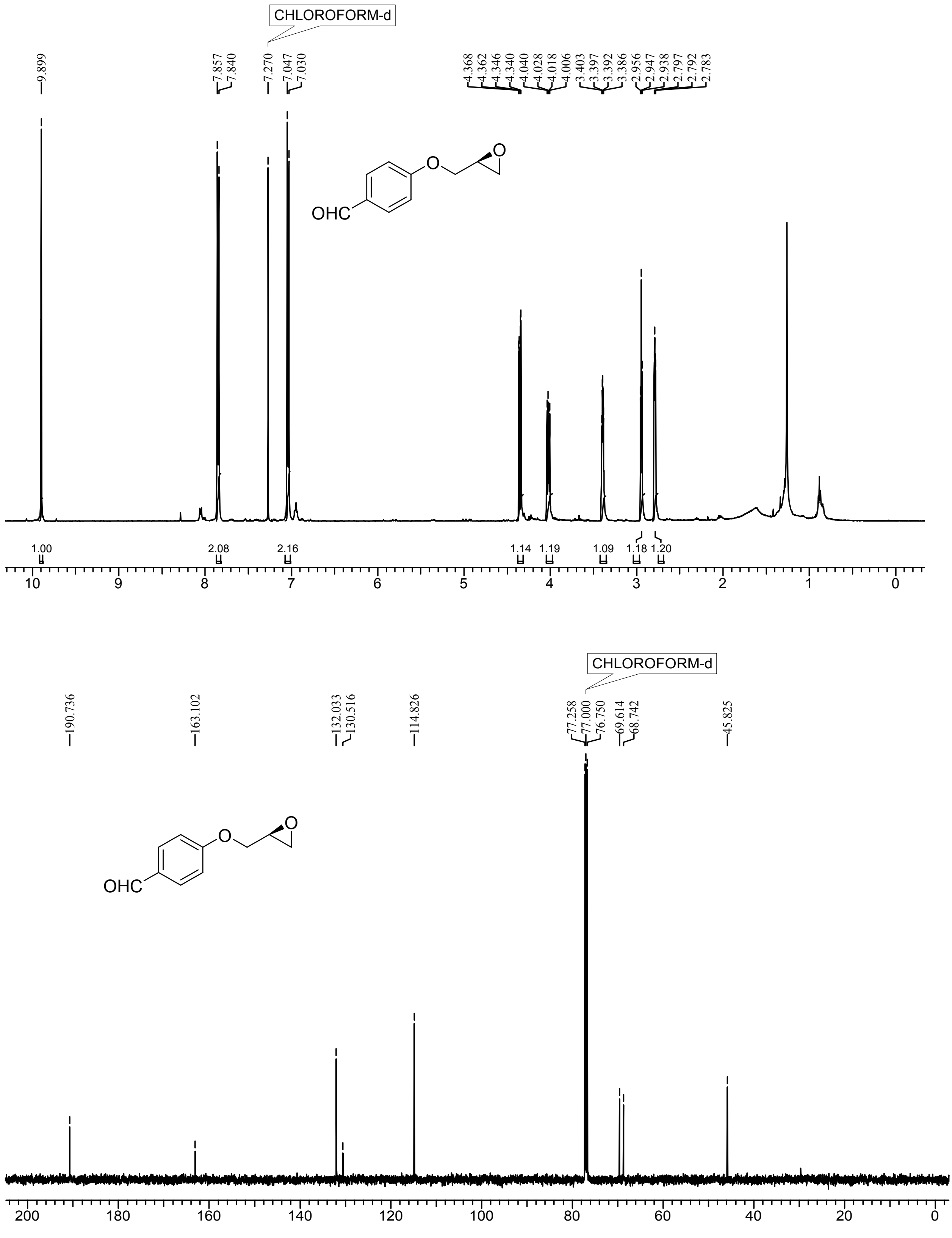

Figure S18: ^{1}H NMR & ^{13}C NMR of (*S*)-4-(oxiran-2-ylmethoxy)benzldehyde.

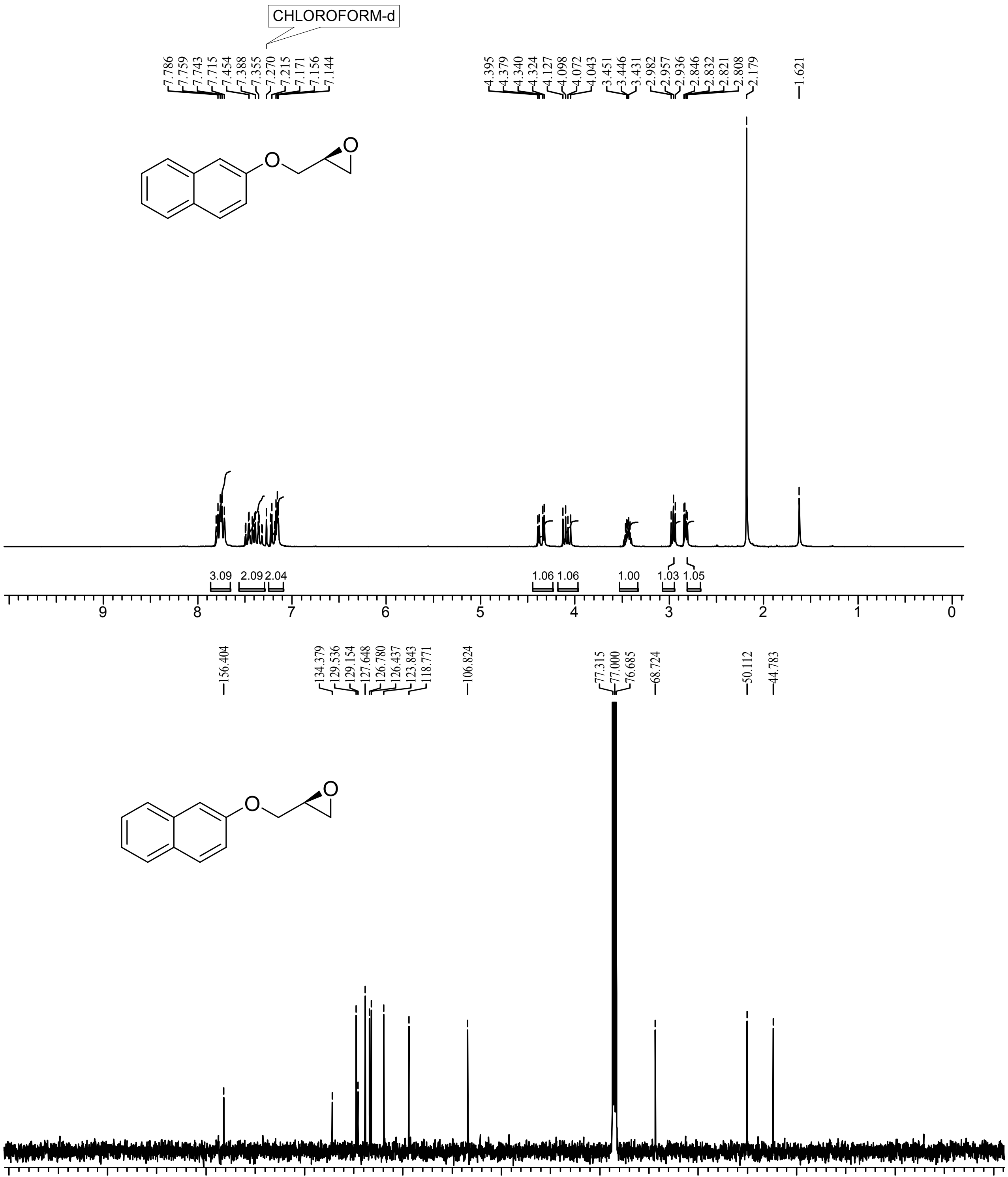

Figure S19: ^{1}H and ^{13}C NMR 2-[naphthalene-2-yloxy)methyl]oxirane

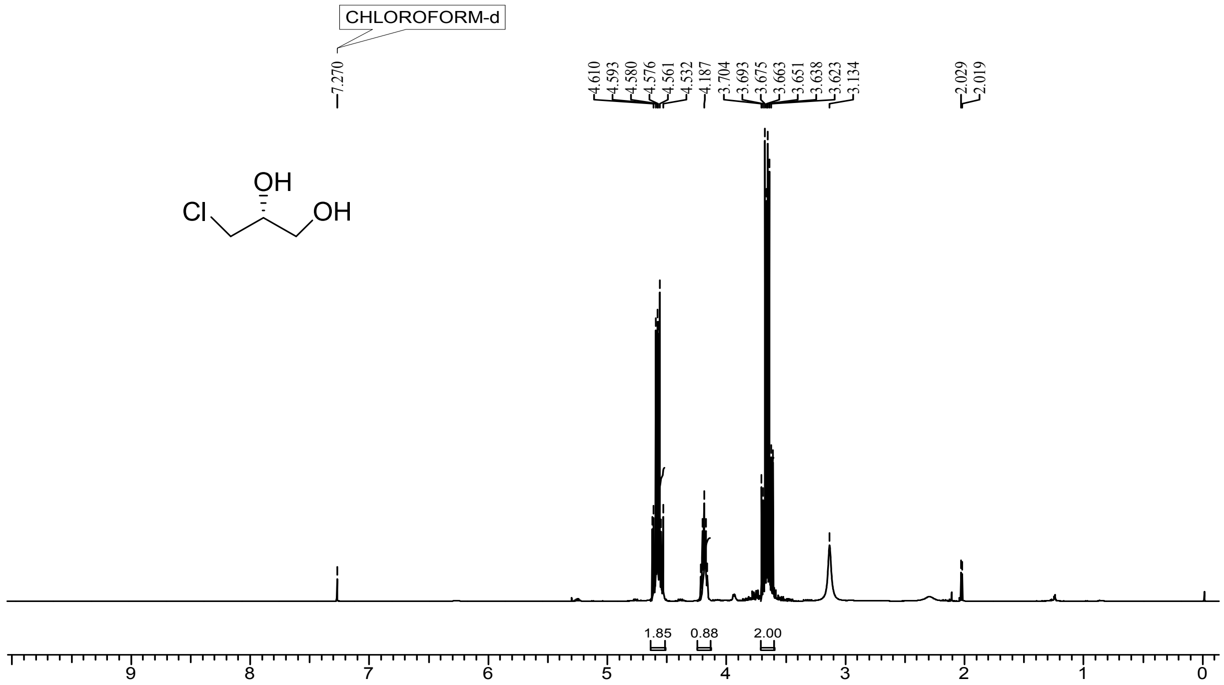

^{13}C NMR

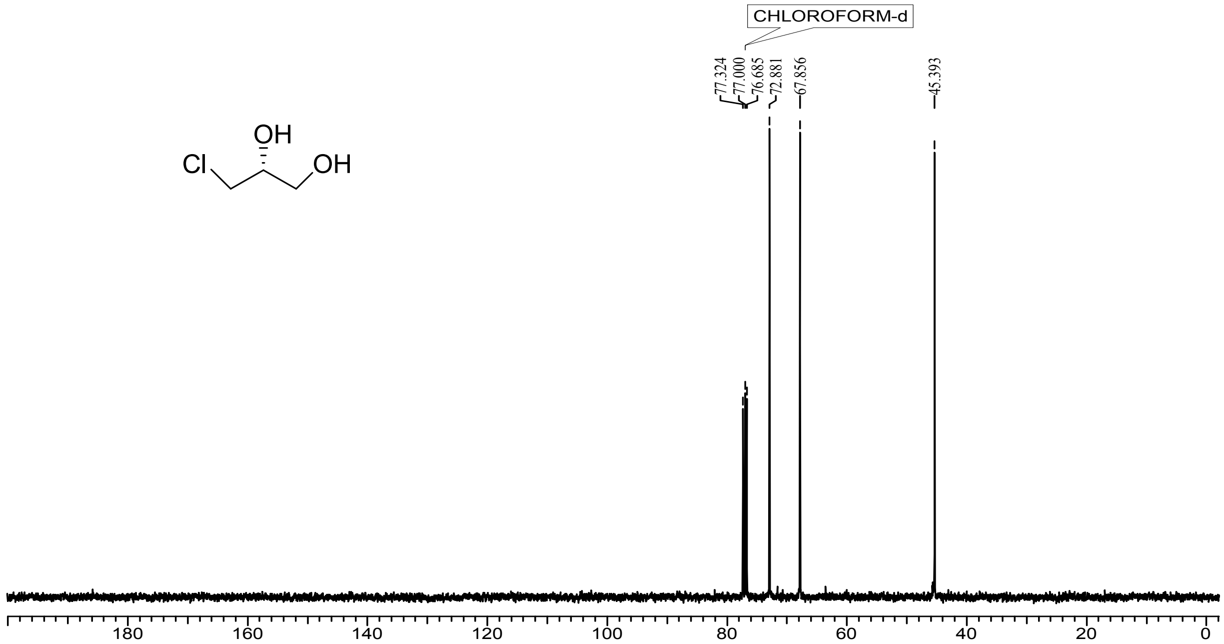

Figure S20: ^{1}H and ^{13}C NMR (*R*)-3-chloropropane-1,2-diol

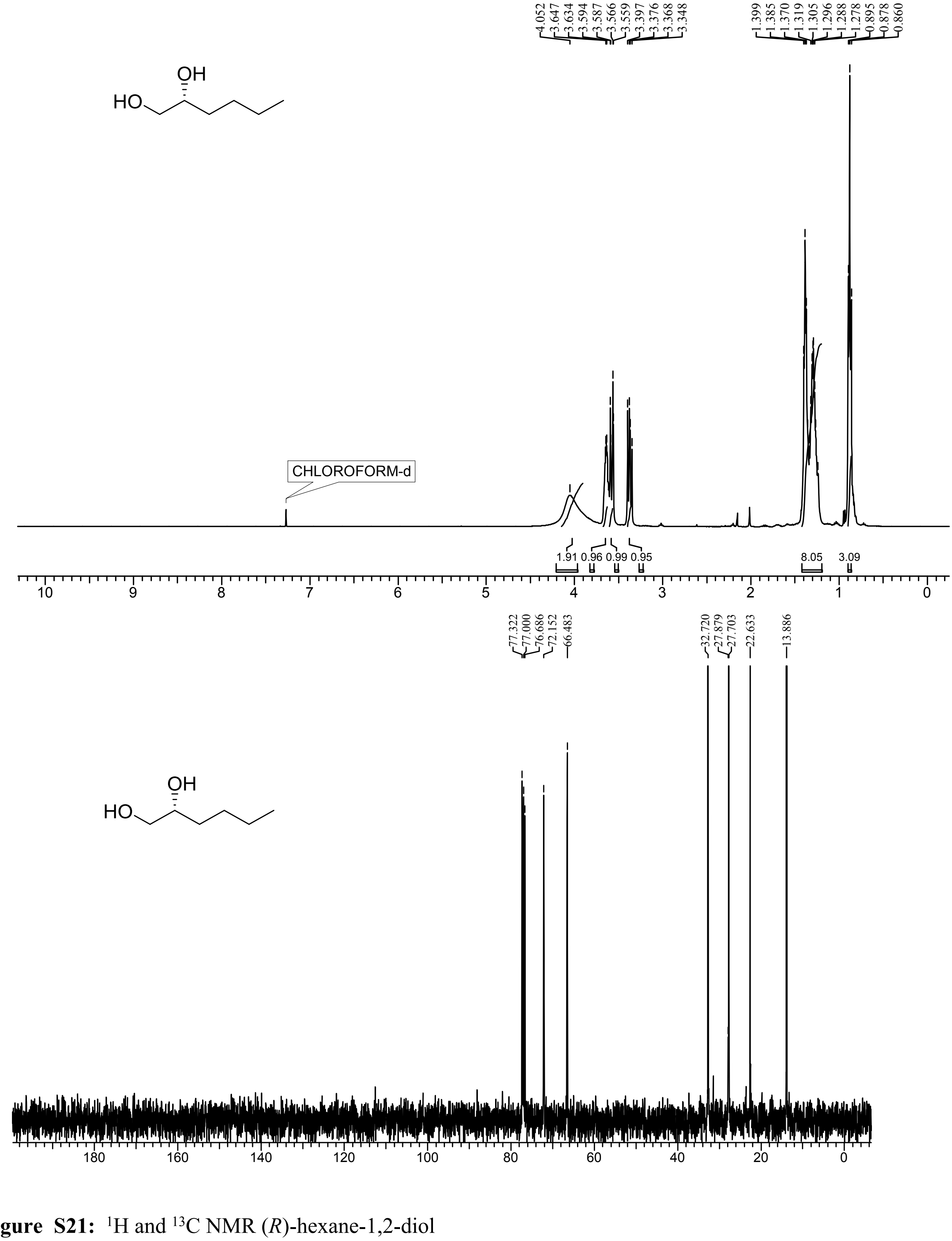

Figure S21: ^{1}H and ^{13}C NMR (*R*)-hexane-1,2-diol

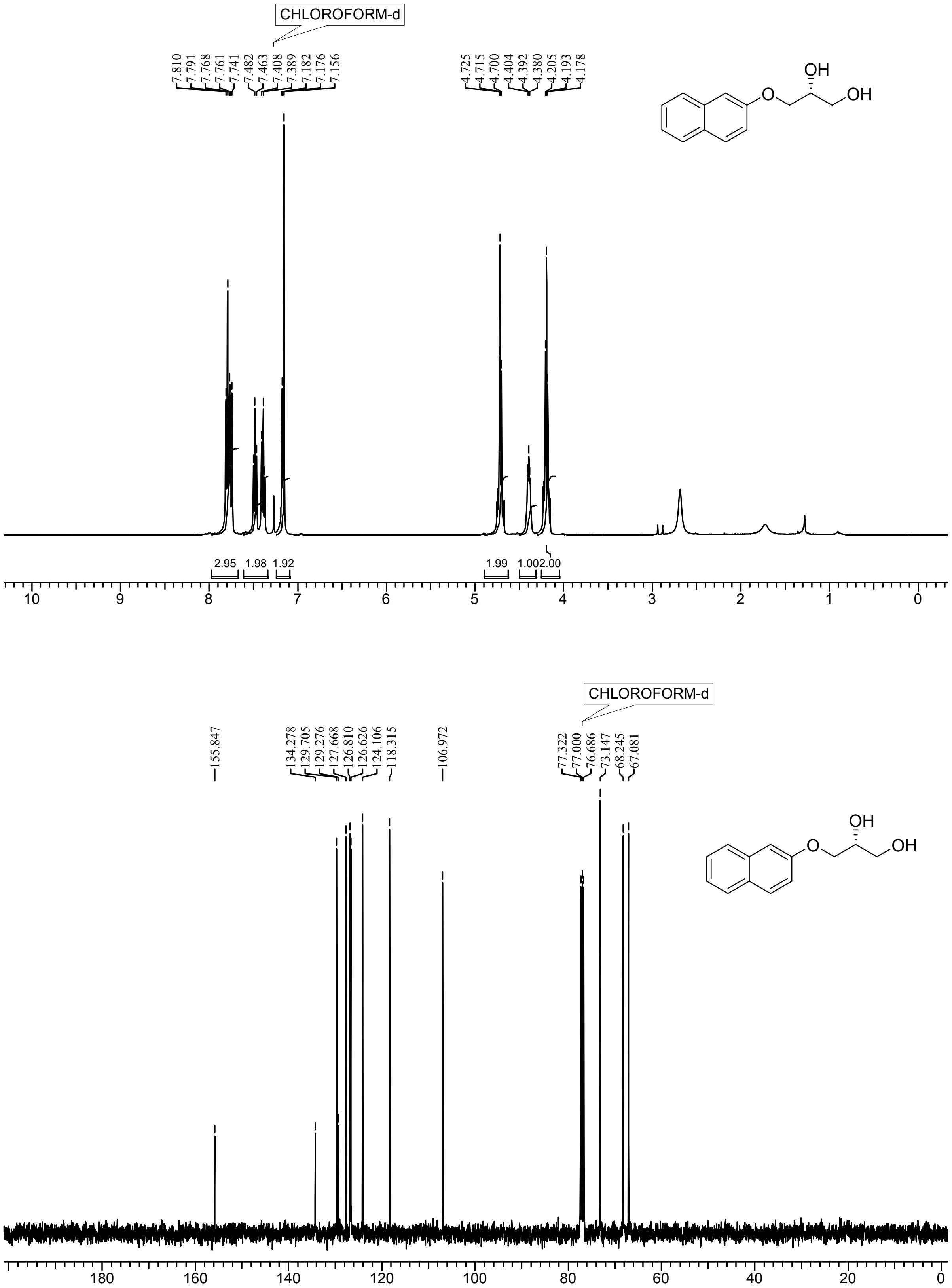

Figure S22: ^{1}H & ^{13}C NMR (*R*)-3-(naphthalene-2-yloxy)propane-1,2-diol

VIII Gas chromatogram of recovered epoxides and diols

G-TA chiral column (Astec® Chiraldex® 30 m × 0.25 mm x 0.12 µm)
50°C isothermal; Flow: 1 ml/min
t_R = 16.038 min. (*S*-ECH) t_R = 17.154 min. (*R*-ECH)

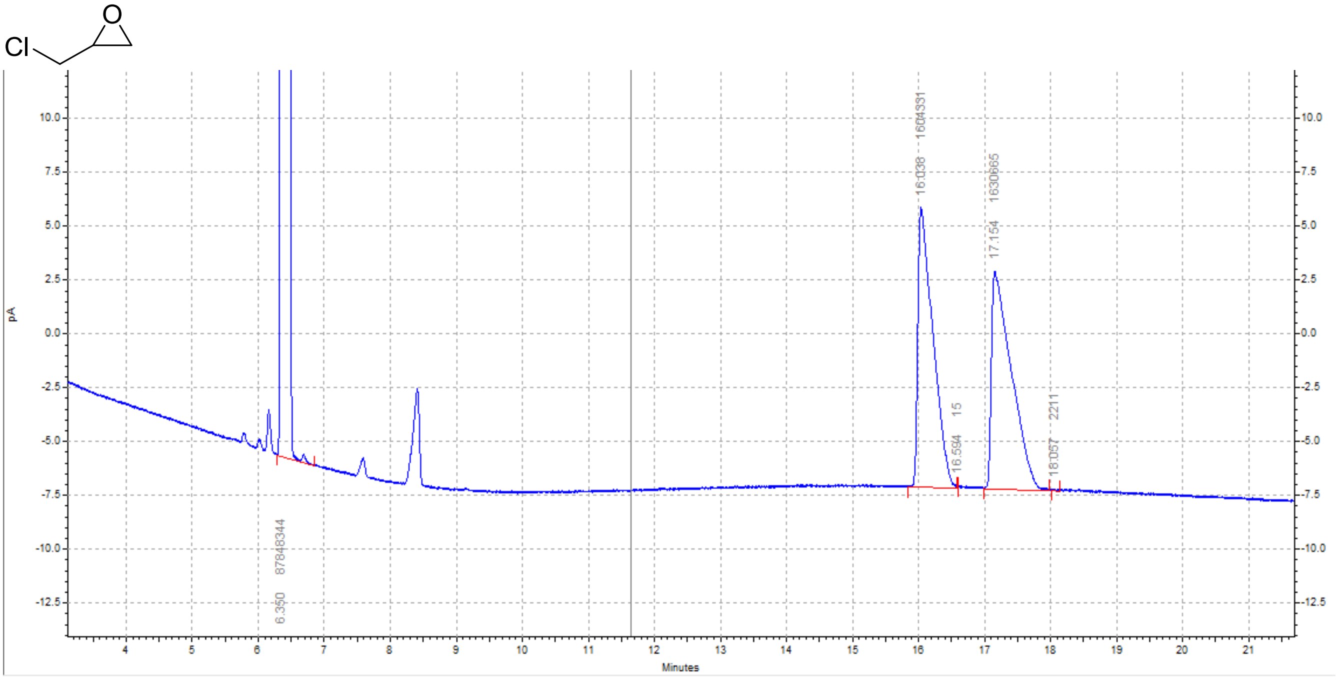

Front Signal
Results

Retention Time	Area	Area %	Height	Height %
6.350	87848344	96.45	18512473	99.04
16.038	1604331	1.76	99980	0.53
16.594	15	0.00	153	0.00
17.154	1630665	1.79	77759	0.42
18.057	2211	0.00	614	0.00
Totals	91085566	100.00	18690979	100.00

Figure S23: Chiral resolution *rac*-epichlorohydrin

G-TA chiral column (Astec® Chiraldex® 30 m × 0.25 mm x 0.12 µm)
50°C isothermal; Flow: 1 ml/min

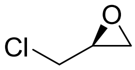

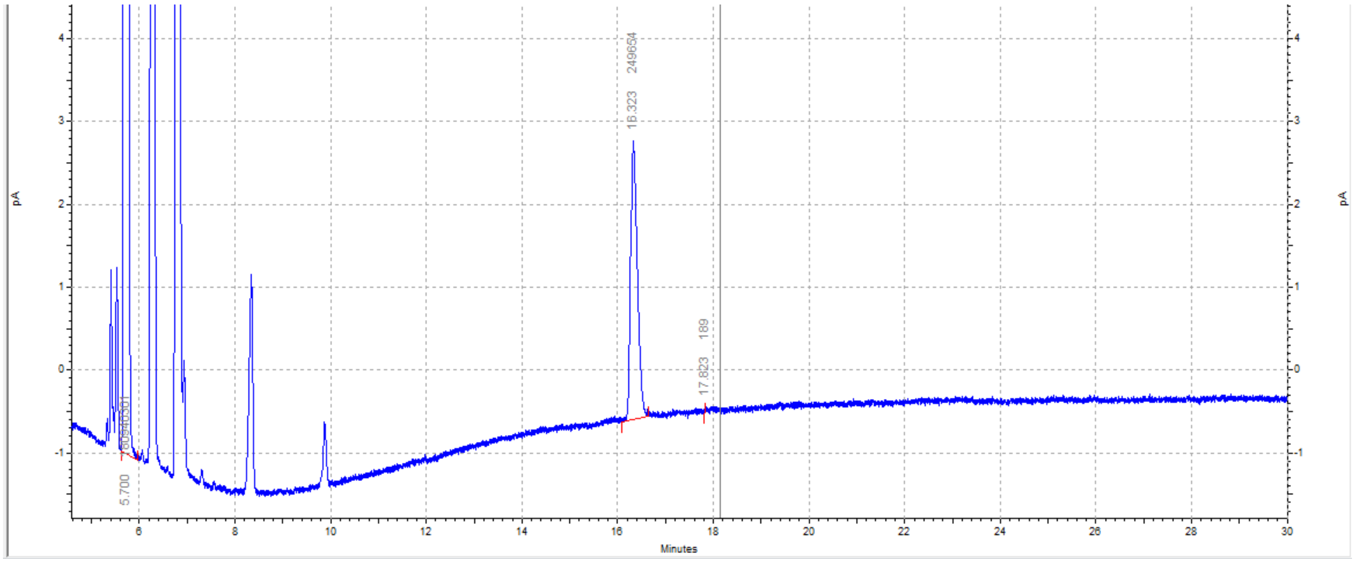

Front Signal
Results

Retention Time	Area	Area %	Height	Height %
5.700	180940301	99.86	63802305	99.96
16.323	249654	0.14	25823	0.04
17.823	189	0.00	466	0.00
Totals	181190144	100.00	63828594	100.00

Figure S24: Analysis of enantioselectivity of ECH

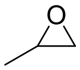

Chiral GC (α-TA , 80 ^{0}C , 5 min, 2 ^{0}C /min to 120 ^{0}C)

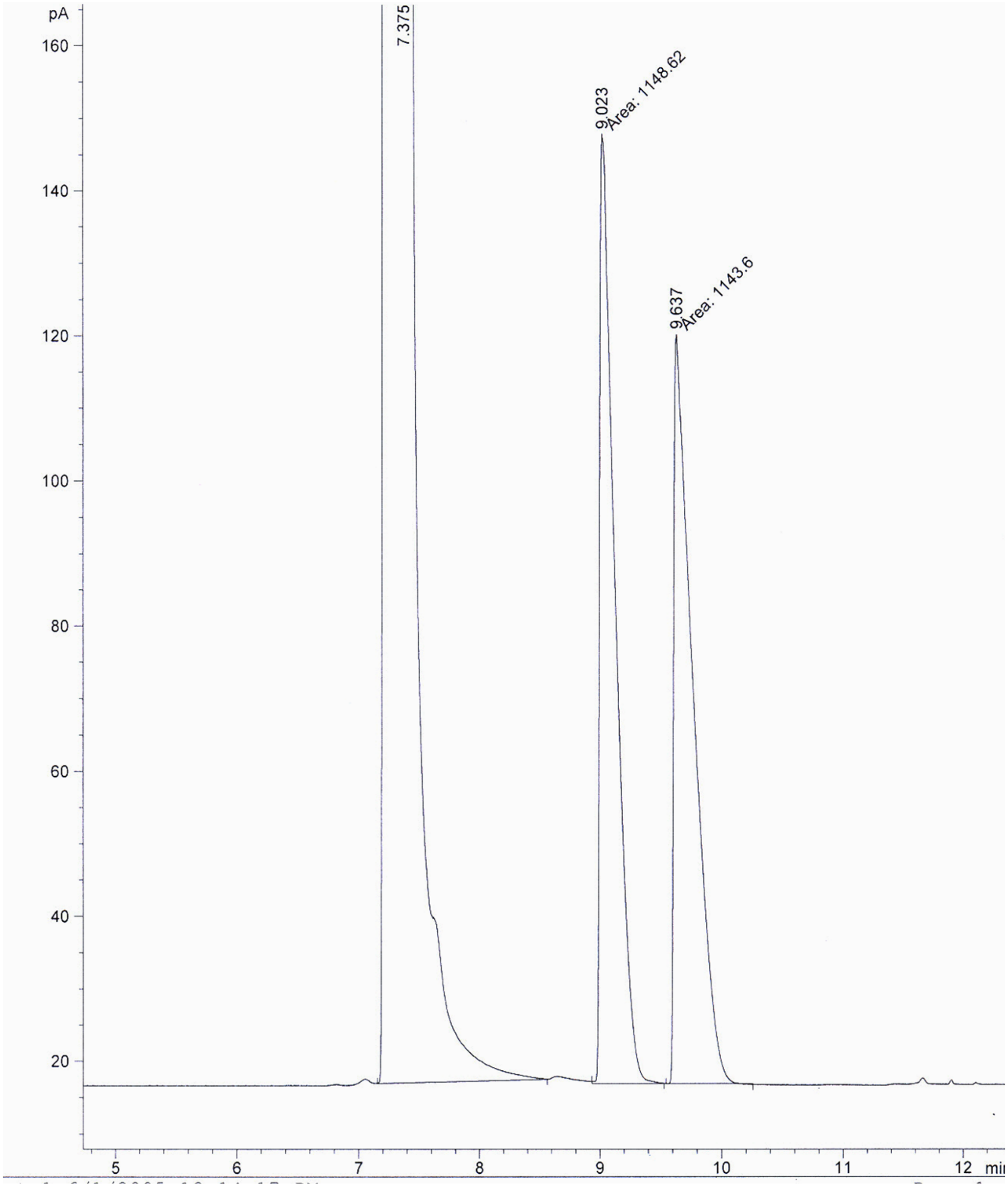

Figure S25: GC of *rac*-2-methyl oxirane

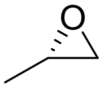

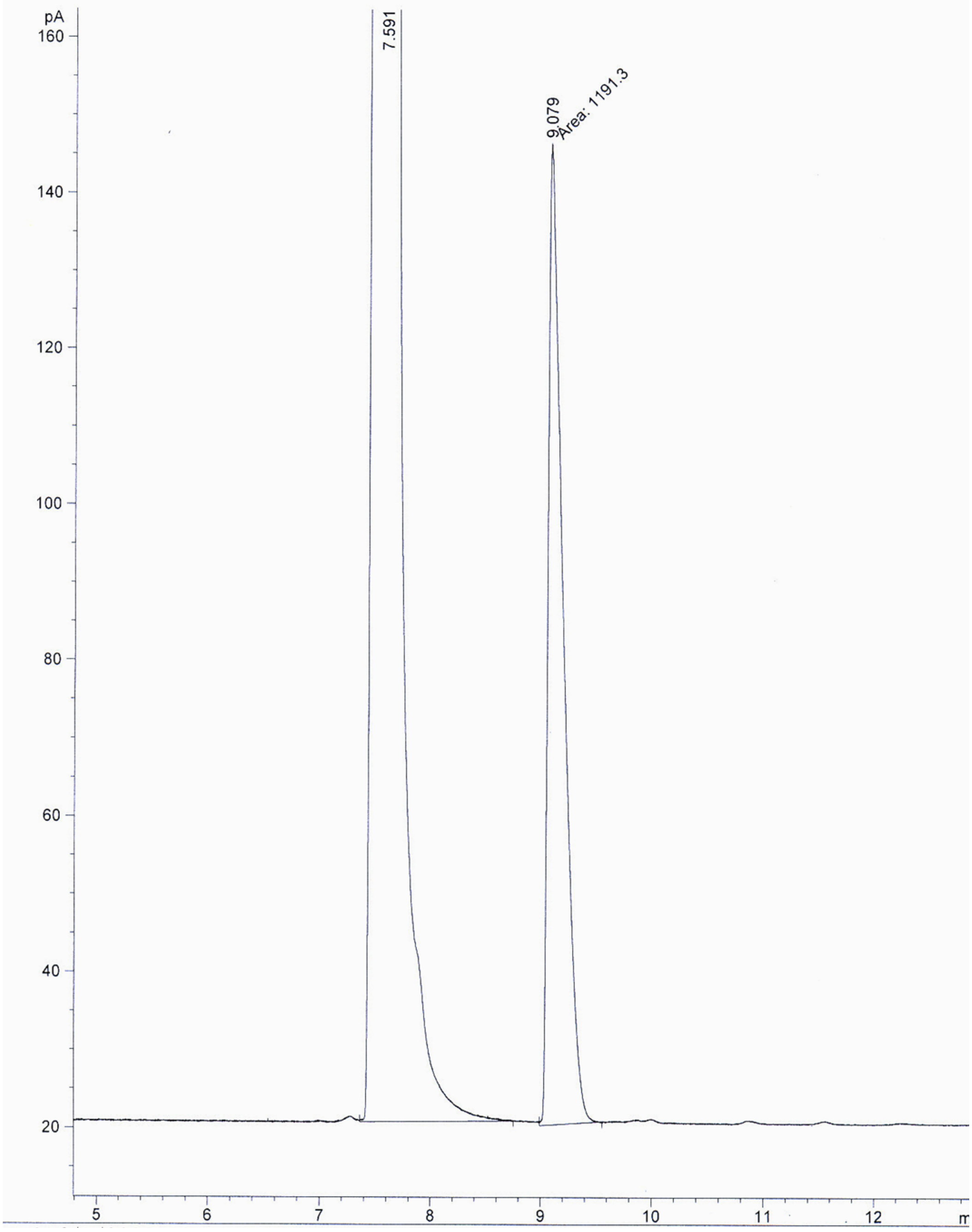

Figure S26: GC of optically active 2-methyl oxirane

γ-TA , 55 ^{0}C ,10min,1 ^{0}C /min to 65 ^{0}C

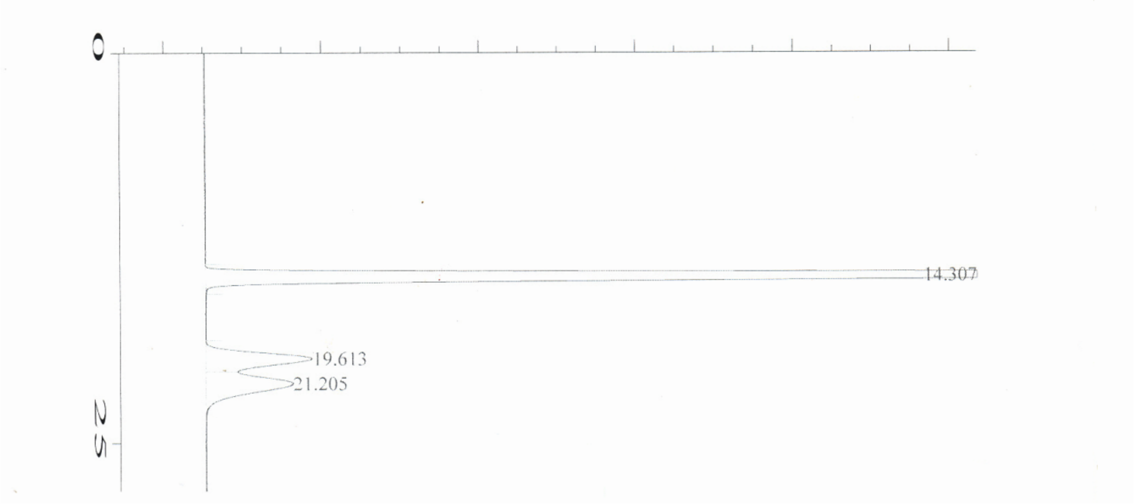

Figure S27: GC of *rac* 2-butyl oxirane

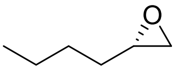

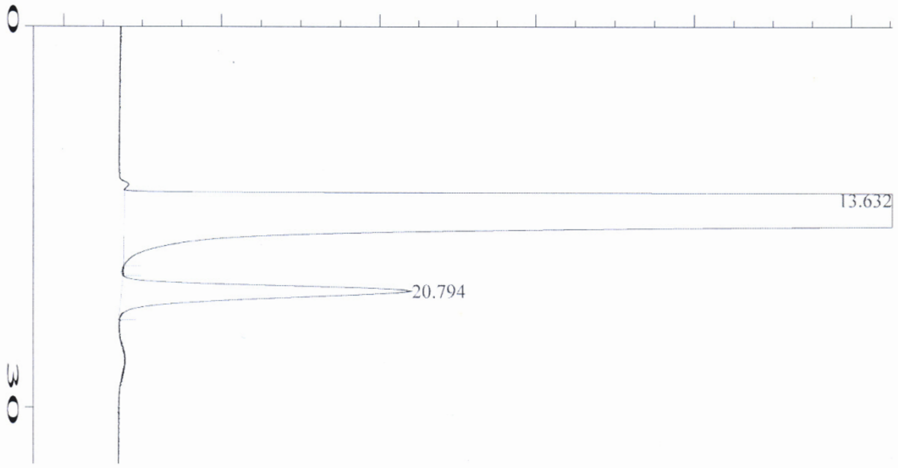

Figure S28: GC of optically active 2-butyl oxirane

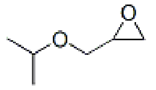

(Chiraldex 20m x 0.25mm γ-TA, 80 ^{0}C, 5min, 2 ^{0}C /min to 100 ^{0}C).

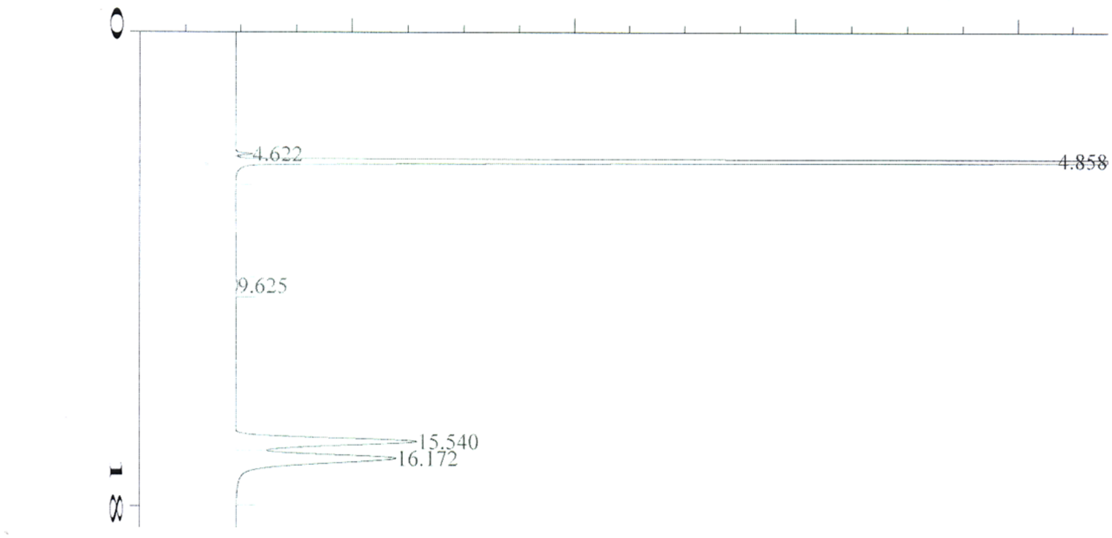

Figure S29: GC of *rac* 2-(isopropoxymethyl)oxirane

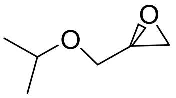

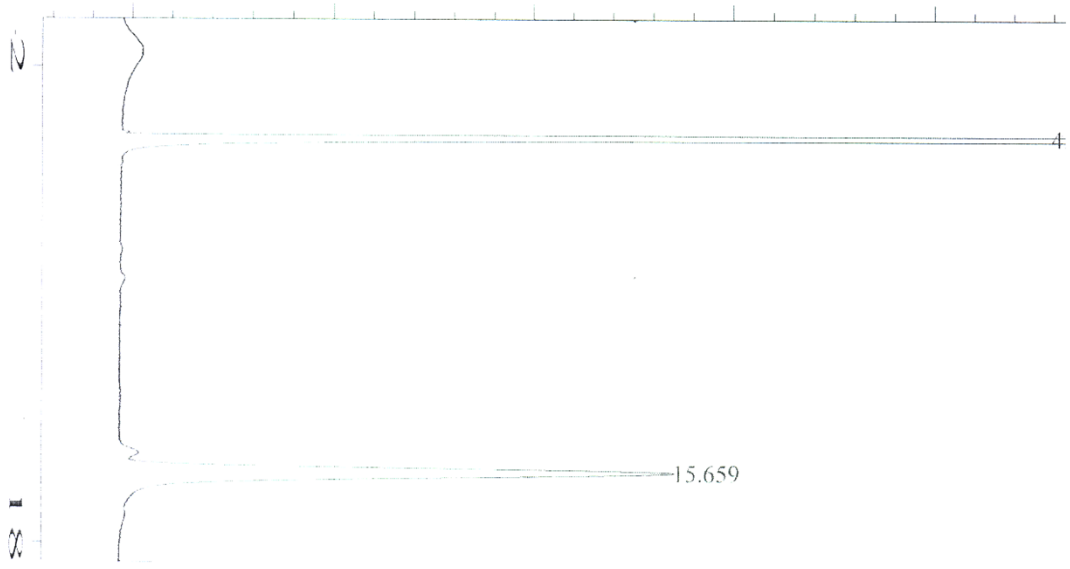

Figure S30: GC of optically active 2-(isopropoxymethyl)oxirane

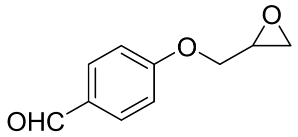

Chiralcel^R OD-H, 20% isopropyl alcohol in n- hexanes, 254 nm, 1 mL/min

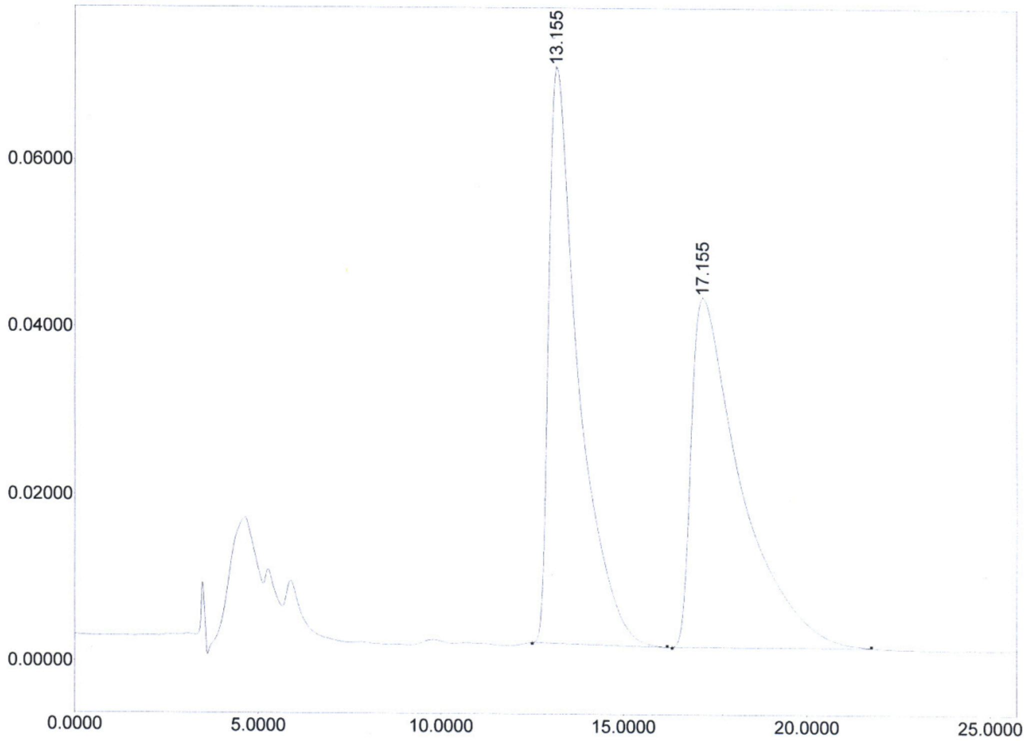

Figure S31: HPLC of *rac* 4-(oxiran-2-ylmethoxy)benzaldehyde

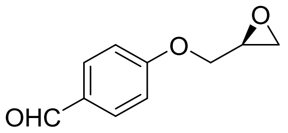

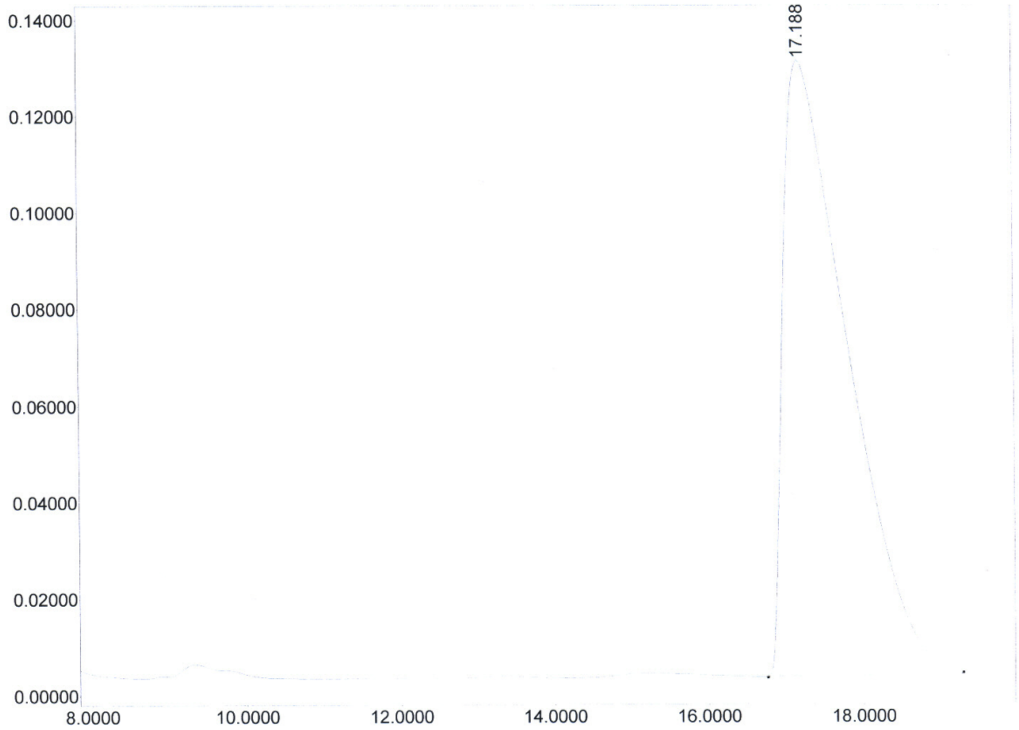

Figure S32: HPLC of optically active 4-(oxiran-2-ylmethoxy)benzaldehyde

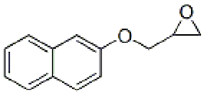

Chiralcel^R OD-H, 10% isopropyl alcohol in n- hexanes, 254 nm, 1 mL/min

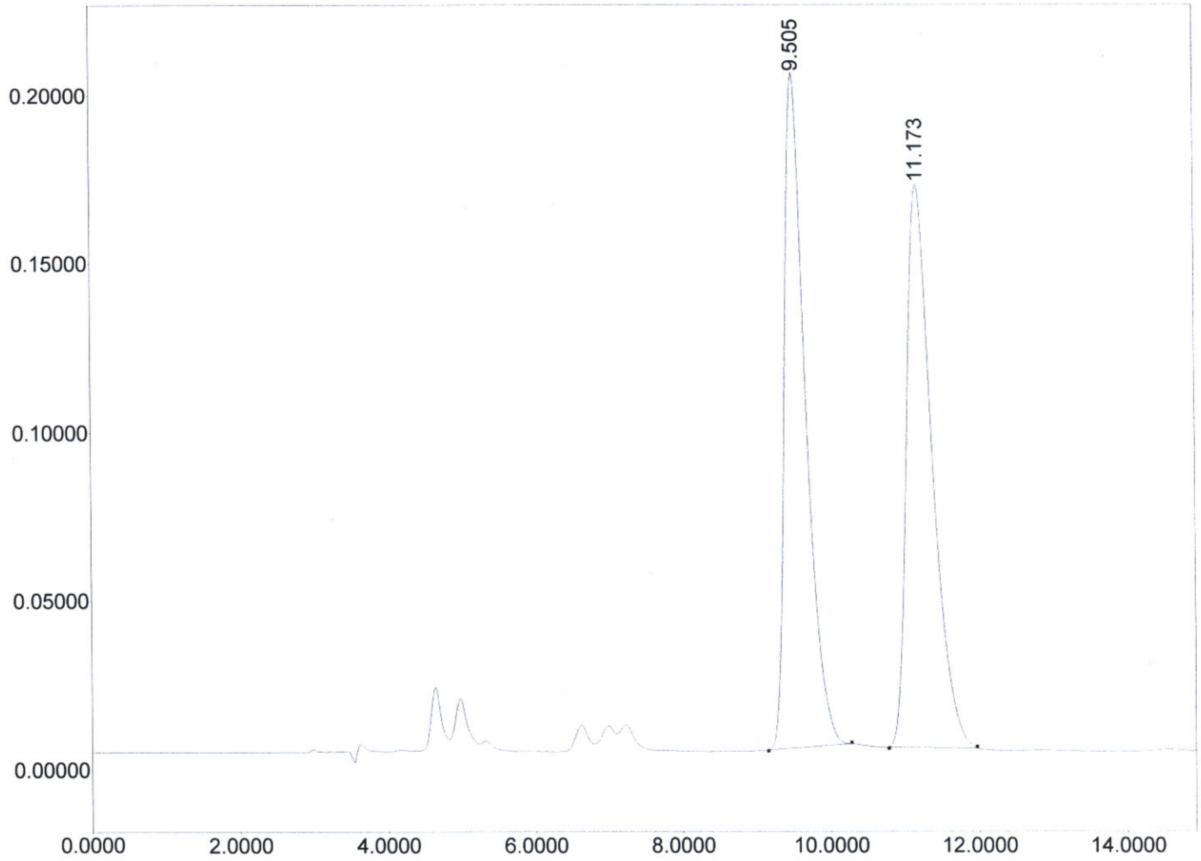

Figure S33: HPLC of *rac* 2-((naphthalen-2-yloxy)methyl)oxirane.

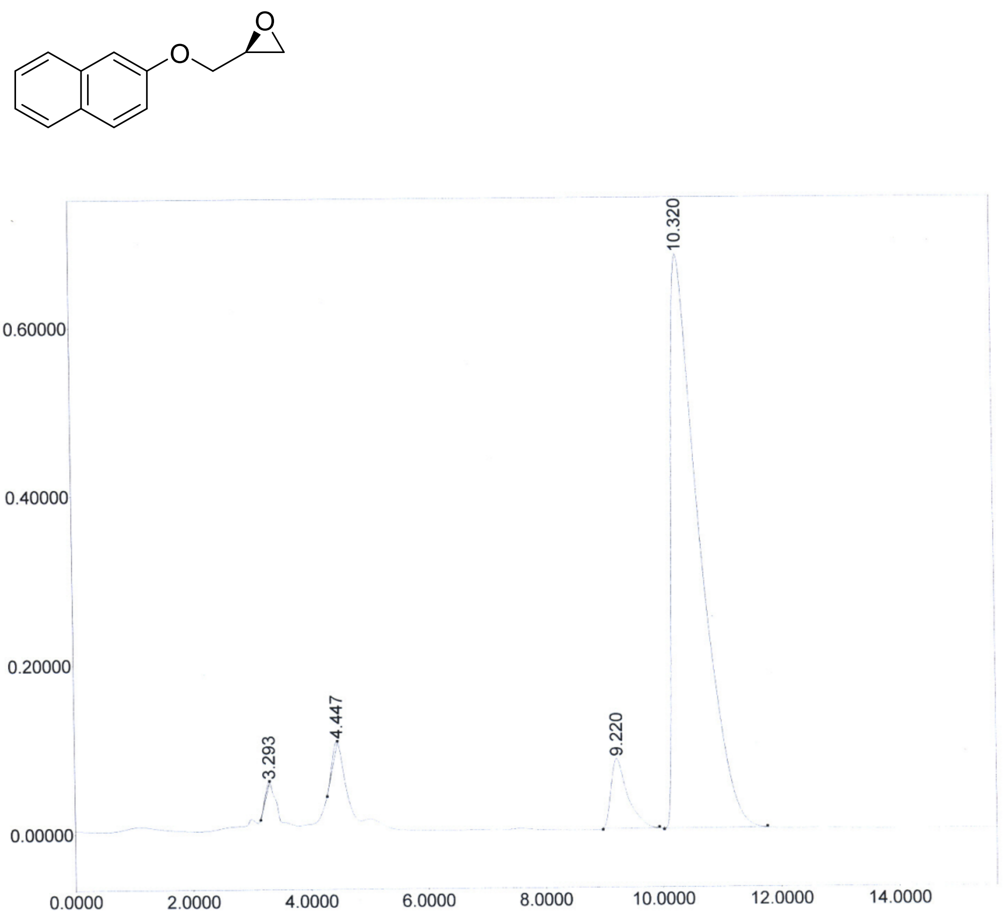

Figure S34: HPLC of optically active 2-((naphthalen-2-yloxy)methyl)oxirane.

IX
Recycling method:

After the completion of HKR reaction of epichlorohydrin (ECH) the resolved ECH and diol were separated through distillation process using Kugelrohr distillation apparatus. The non volatile residue dimer catalyst B which became partly reduced from Co(III) to Co(II) could again reactivated by 0.66 equiv. of $Y(OTf)_3$ and reused as per the above mentioned reaction method.

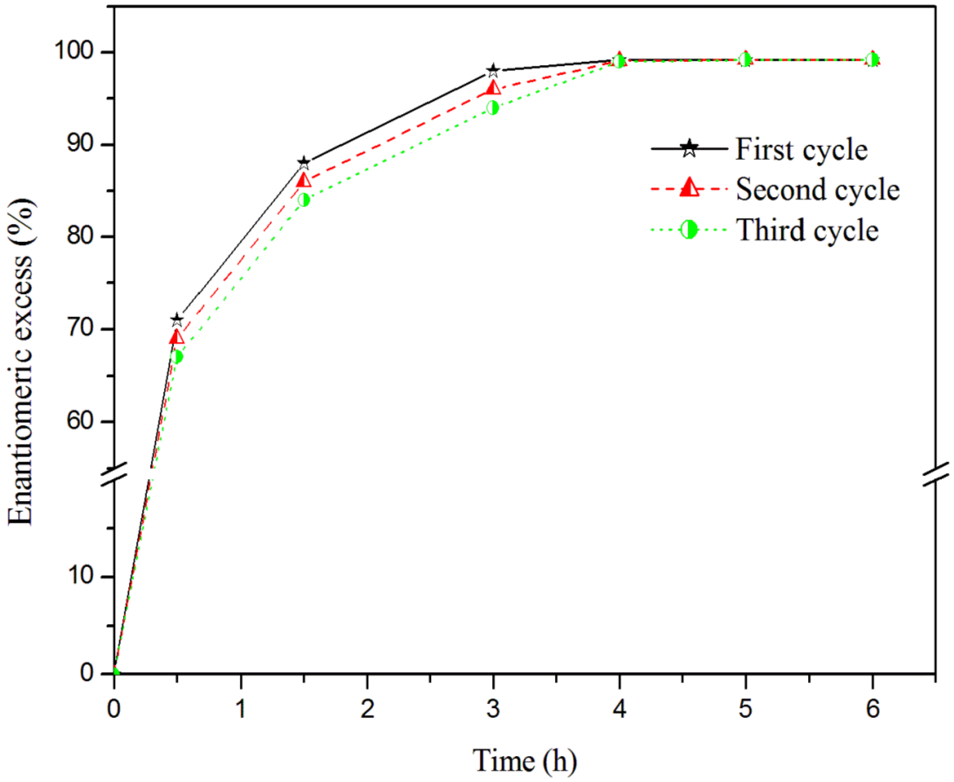

Figure S35 : Recyclability of the chiral salen Co- $Y(OTf)_3$ dimer catalyst B in the enantioselective HKR of (±) ECH using 0.2 mol % catalyst at room temperature.

X

References:

1. R.G. Konsler, J Karl and E.N. Jacobsen, *J. Am. Chem. Soc.*1998,**120**, 10780-10781.
2. R. Breinbauer and E.N. Jacobsen, *Angew. Chem. Int. Ed*. 2000, **39**, 3604-3607.
3. S. S. Thakur, W. Li, S.-J. Kim and G.-J. Kim *Tetrahedron Lett.* 2004, **45**, 7429-7433.
4. S. S. Thakur , S.W. Chen , W. Li , C.K. Shin, S. J. Kim, Y. M Koo, G. J. Kim *J Organomet. Chem.* 2006, **691**, 1862–1872.
5. C. M. Liao, C. C. Hsu, F.S. Wang, B. B. Wayland and C.H. Peng , *Polym. Chem.*, 2013, **4**, 3098–3104.